AD-A060 600 AIR FORCE FLIGHT DYNAMICS LAB WRIGHT-PATTERSON AFB OHIO F/G 20/4
BOUNDARY LAYER FENCE METHOD FOR MEASURING SURFACE SHEAR STRESS --ETC(U)
AUG 78 A W FIORE, N E SCAGGS

UNCLASSIFIED AFFDL-TR-78-89 NL

1 OF 1

AD
A060600

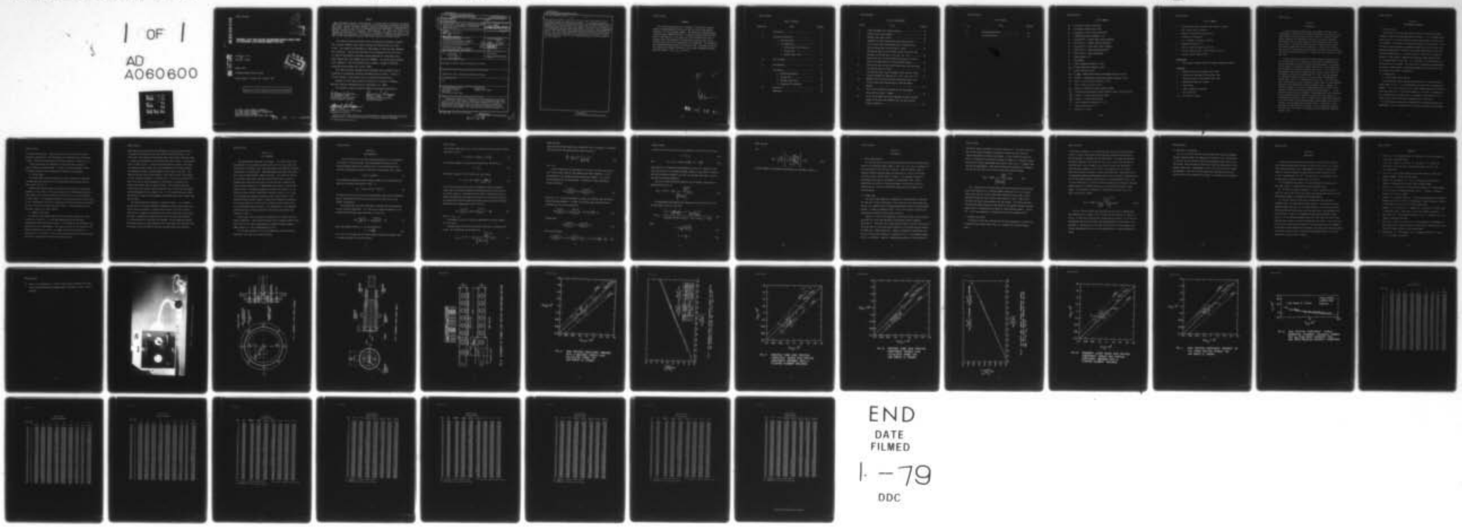

END
DATE
FILMED
1-79
DDC

AFFDL-TR-78-89

BOUNDARY LAYER FENCE METHOD FOR MEASURING SURFACE SHEAR STRESS IN A SUPERSONIC, HIGH REYNOLDS NUMBER FLOW FIELD

Anthony W. Fiore
and
Norman E. Scaggs

August 1978

TECHNICAL REPORT AFFDL-TR-78-89

Interim Report - October 1977 to April 1978

Approved for Public Release; Distribution Unlimited

AIR FORCE FLIGHT DYNAMICS LABORATORY
AIR FORCE WRIGHT AERONAUTICAL LABORATORIES
AIR FORCE SYSTEMS COMMAND
WRIGHT-PATTERSON AIR FORCE BASE, OHIO 45433

NOTICE

This report contains the results of an investigation undertaken to develop the so-called "boundary layer fence" technique for obtaining the wall shear stress. The research was conducted at a Mach number of three for near adiabatic wall conditions. The work was performed in the Aeromechanics Division of the Air Force Flight Dynamics Laboratory, Wright-Patterson Air Force Base, Ohio, under Project 2307, Task 2307Ø4, Work Unit 23070424. The research was performed by Dr. Anthony W. Fiore of AFFDL/FXE and Mr. Norman E. Scaggs of AFFDL/FXG during the period October 1977 to April 1978.

This report has been reviewed by the Information Office,(ASD/OIP) and is releasable to the National Technical Information Service (NTIS). At NTIS, it will be available to the general public, including foreign nationals.

Requests for this report should be directed to: U.S.Dept. of Commerce, National Technical Information Service, Washington, D.C. 20230.

This technical report has been reviewed and approved for publication.

Anthony W. Fiore

Dr. Anthony W. Fiore
Aeromechanics Division/AFFDL
Senior Research Scientist

Norman E. Scaggs

Norman E. Scaggs
Aeromechanics Division/AFFDL
Aerospace Engineer

Alfred C. Draper

ALFRED C. DRAPER
Assistant for Research & Technology
Aeromechanics Division

AIR FORCE/56780/20 September 1978 — 400

REPORT DOCUMENTATION PAGE

READ INSTRUCTIONS BEFORE COMPLETING FORM

1. ~~REPORT NUMBER~~ (14) AFFDL-TR-78-89	2. GOVT ACCESSION NO.
3. RECIPIENT'S CATALOG NUMBER (9)	
4. ~~TITLE (and Subtitle)~~ (6) BOUNDARY LAYER FENCE METHOD FOR MEASURING SURFACE SHEAR STRESS IN A SUPERSONIC, HIGH REYNOLDS NUMBER FLOW FIELD	5. TYPE OF REPORT & PERIOD COVERED Interim Report, October 1977 ~~to~~ April 1978
	6. ~~PERFORMING ORG.~~ REPORT NUMBER
7. AUTHOR(s) (10) ~~Dr.~~ Anthony W. Fiore ~~and~~ ~~Mr.~~ Norman E. Scaggs	8. CONTRACT OR GRANT NUMBER(s)
9. PERFORMING ORGANIZATION NAME AND ADDRESS Aeromechanics Division, Air Force Flight Dynamics Laboratory, Wright-Patterson AFB, Ohio 45433	10. PROGRAM ELEMENT, PROJECT, TASK AREA & WORK UNIT NUMBERS (16) 2307Ø424 (17) Ø4
11. CONTROLLING OFFICE NAME AND ADDRESS Aeromechanics Division, Air Force Flight Dynamics Laboratory, Wright-Patterson AFB, Ohio 45433	12. REPORT DATE (11) August 1978
	13. NUMBER OF PAGES 48
14. MONITORING AGENCY NAME & ADDRESS (if different from Controlling Office) N/A (12) 48p.	15. SECURITY CLASS. (of this report) Unclassified
	15a. DECLASSIFICATION/DOWNGRADING SCHEDULE

16. DISTRIBUTION STATEMENT (of this Report)

Approved for public release; distribution unlimited.

17. DISTRIBUTION STATEMENT (of the abstract entered in Block 20, if different from Report)

Approved for public release; distribution unlimited.

18. SUPPLEMENTARY NOTES

N/A

19. KEY WORDS (Continue on reverse side if necessary and identify by block number)

Turbulent boundary layers
High Reynolds Numbers
Supersonic
Skin friction coefficient
Preston tube
Boundary layer fence

20. ABSTRACT (Continue on reverse side if necessary and identify by block number)

Experimental research on a boundary layer fence technique was conducted in the Air Force Flight Dynamics Laboratory's M=3 high Reynolds number wind tunnel located in bldg. 450, area B of Wright-Patterson Air Force Base, Ohio. The purpose of the research was to develop this particular technique for measuring the surface shear stress in a supersonic compressible turbulent boundary with near adiabatic wall condition and zero pressure gradient. The

Ø12Ø7Ø

1B

Item #20 ABSTRACT (Cont'd)

20,000 540,000

measurements were made on the tunnel wall at a nominal Mach number of three. The Reynolds number was changed by two methods, i.e., changing the tunnel stagnation pressure and the measuring station. The resulting momentum thickness Reynolds number varied from 2×10^4 to approximately 54×10^4. The recorded measurements were (a) the surface shear stress, (b) the Preston pressures, and (c) the pressures ahead and behind the boundary layer fence. The corresponding skin friction coefficients were compared with each other and the Van Driest II theory. The skin friction coefficients obtained with the fence agreed reasonably well with those obtained with a balance and the Preston tube. The skin friction coefficients from all three techniques agreed very well with the Van Driest II theory.

FOREWORD

This report was prepared by Dr. Anthony W. Fiore and Mr. Norman E. Scaggs of the Aeromechanics Division of the Air Force Flight Dynamics Laboratory, Air Force Systems Command. The research was conducted under work unit number 23070424 entitled, "Viscous and Interacting Flow Fields about Flight Vehicles." This particular effort concerns itself with a boundary layer fence technique for measuring the surface shear stress from which the skin friction coefficient can be obtained. The experiments were performed between October 1977 and April 1978. They were carried out at a nominal Mach number of three and in the range of momentum thickness Reynolds numbers $2 \times 10^4 \leq R_{e_\theta} \leq 54 \times 10^4$.

TABLE OF CONTENTS

LIST OF ILLUSTRATIONS

LIST OF TABLES

LIST OF SYMBOLS

A_0 = Calibration constant see eq.(3)

B_0 = Calibration constant see eq.(3)

C_f = $\tau_{w_g}/\frac{1}{2}\rho_e U_e^2$ = Skin friction coefficient

d = Preston tube outside diameter in ft.

F_3 = $\tau_{w_g} \cdot d^2/4\rho^* \nu^{*2}$ = Preston shear stress parameter

F_4 = $\overline{\Delta P}_p \cdot d^2/4\rho^* \nu^{*2}$ = Preston pressure parameter

F_5 = $\tau_{w_g} \cdot h^2/4\rho^* \nu^{*2}$ = Fence shear stress parameter

F_6 = $\Delta P_f \cdot h^2/4\rho^* \nu^{*2}$ = Fence pressure parameter

F_7 = $\overline{\Delta P}_p \cdot h^2/4\rho^* \nu^{*2}$ = Coupling parameter

h = Fence height in ft.

M = Mach number

P_0 = Tunnel stagnation pressure in psia

P_{p_t} = Preston tube total pressure in psia

P = Static pressure in psia

$\overline{\Delta P}_p$ = $\frac{\gamma}{2} P_w M_p^2$ = Compressible Preston tube dynamic pressure in psia

ΔP = $P_{p_t} - P_w$ = Incompressible Preston tube dynamic pressure in psia

ΔP_f = $P_f - P_b$ = Fence pressure difference in psia

q = $\frac{\gamma}{2} p M^2$ = Dynamic pressure in psia

R_{e_θ} = $\rho_e U_e \theta/\mu_e$ = Momentum thickness Reynolds number

$\overline{R}_{e_\theta}$ = Incompressible momentum thickness Reynolds number given by eq.(21)

$R_{e_d}^*$ = $\rho^* U_e d/\mu^*$ = Preston tube Reynolds number

$R_{e_h}^*$ = $\rho^* U_e h/\mu^*$ = Fence Reynolds number

T_0 = Tunnel stagnation temperature in °R

T = Static temperature in °R

U = Velocity in ft/sec.

LIST OF SYMBOLS

X = Distance from tunnel throat to test station in inches

τ = tau = shear stress in lbs/ft^2

ρ = Density in $slugs/ft^3$ or $lbs.sec^2/ft^4$

μ = Viscosity in $lbs.sec/ft^2$

ν = μ/ρ = kinematic viscosity in ft^2/sec.

θ = Momentum thickness in ft.

γ = Ratio of specific heats (1.4 for air)

R = The gas constant taken as 1715 ft^2/sec^2 °R for air

r = Recovery factor taken as 0.88

Superscripts

$*$ = Value based on Sommer and Short reference temperature method

Subscripts

b = Conditions behind the boundary layer fence

e = Conditions at the edge of the boundary layer

f = Conditions ahead of the boundary layer fence

g = Measurements made with a gauge

p = Preston tube

0 = Tunnel stagnation conditions

w = Wall conditions

V.D. = Van Driest II theory

SECTION I

INTRODUCTION

In most aeronautical applications a knowledge of the total drag created when an aircraft moves through the atmosphere is essential to the understanding of the performance of such a vehicle. Because of recent energy shortages, this knowledge is becoming increasingly important. Considerable effort has been devoted to the measurement of the surface shear stress in the hope that the total drag of these vehicles can be decreased by reducing the skin friction drag. Eventually it is hoped that the skin friction drag can be controlled in order to either conserve fuel for a given flight condition or increase the flight range for a given fuel load.

Prior to conducting research on various methods for decreasing the skin friction drag, it is necessary to develop the instrumentation and testing techniques required for making these measurements. The purpose of this report is to describe a method referred to as the boundary layer fence technique for obtaining the wall shear stress. In all probability the boundary layer fence for measuring the wall shear stress was first introduced by Konstantinov and Dragnysh[10] in 1955. The same technique was employed by Vagt and Fernholz[11] to measure the three-dimensional surface shear stress in an incompressible flow field. Like the Preston tube,[1] the fence can be used to obtain the shear stress in a non-separated compressible two-dimensional turbulent boundary layer.[5] However, its greatest advantage is its use in a three-dimensional flow field in the presence of both strong pressure gradients and separation.[5,11] In this experiment the fence was calibrated in a two-dimensional flow field based on the assumption that the resultant surface shear stress vector in a three-dimensional boundary layer is related to the skewed velocity profile in a similar manner as the two-dimensional surface shear stress vector is related to its two-dimensional velocity profile. The results of this experiment indicate that this technique is a valid method for measuring the local wall shear stress in a compressible two-dimensional turbulent boundary layer.

SECTION II

EXPERIMENTAL APPARATUS

1. The Wind Tunnel

The facility used in the experiment was the Air Force Flight Dynamics Laboratory's Mach 3 high Reynolds number wind tunnel. It is a blowdown wind tunnel with an 8.2 x 8 inch closed test section whose upper and lower walls are contoured. It operates at stagnation pressures of 50 to 600 psia. Since the facility does not possess a stagnation temperature control system, the stagnation temperature is slightly below ambient temperature resulting from the Joule-Thompson effect. At these conditions the facility is capable of operation in the range of freestream unit Reynolds number extending from 10^7 to approximately 10^8 per foot. It is designed to run continuously for a maximum period of 10 minutes. Runs during this investigation averaged about 30 seconds. Further details on operating procedures and calibration of this wind tunnel are available in Reference 2.

2. Instrumentation

a. Surface Shear Stress Balance

The surface shear stress was measured directly with a floating-element balance shown in Fig. 1. It was manufactured by the Kistler Instrumentation Company. It is a self sealed unit with a flat surface permitting flush mounting in the tunnel wall. The floating element is 0.37 inches in diameter and has a peripheral gap of 0.003 inches. The balance is self-nulling to the center position and is statically balanced about all three axes.

During testing, the electrical components were at ambient pressure and temperature. Prior to installation in the tunnel the balance was calibrated

by applying known weights. Before and after each run the calibration was constantly checked with a self-calibration coil contained within the balance housing. The read-out and electronic calibration control is shown in Fig. 1.

Primary concern was the destruction of the balance when exposed to tunnel starting and stopping loads. In order to avoid catastrophic failure the balance retraction system described in Reference 3 was employed.

b. Preston tubes

Two Preston tubes and their related wall static pressure and temperature instrumentation were used to provide a second method for measuring the wall shear stress (see Fig. 2).

These Preston tubes consisted of cylindrical pitot pressure tubes placed tangential to the surface. They were constructed from #304 annealed stainless steel tubing with an outside diameter of 0.062 inches and an inside diameter of 0.0472 inches. The streamwise lengths of these pitot tubes were 0.125 inches. In this investigation a new form of the Keener and Hopkins Preston tube equation[4] was used in arriving at the surface shear stress. This relationship will be described in detail in a later section.

c. Boundary Layer Fence

The design of the boundary layer fence is relatively simple and is shown in both Fig. 2 and Fig. 3. It has been determined that the best fence configuration should have square corners.[5] This feature was incorporated in the design used in this investigation. The fence had a span of 0.2 inches while its height and width was 0.01 inches. On either side of the fence there is a pressure port, in the form of a slot, used to measure the lateral pressures when the fence is aligned with the flow field velocity vector.

These same ports give the pressure differential, $\Delta P_f = P_f - P_b$, when the fence is rotated ninety degrees to the local velocity vector at the wall. The former gives the direction of the surface shear stress vector while the latter is related to the magnitude of the surface shear stress vector. These pressure slots are shown in Fig. 3. They are the same length and width as the fence. The pressures sensed by these slots are transmitted to the proper recording instrumentation through isolated chambers on both sides of the fence. The fence and the main body are fabricated as a unit thus insuring a high degree of fence structural integrity. As shown in Fig. 2 this unit is placed in the base of the test plate and attached to a shaft which is connected to an external drive motor used to rotate the fence. The previously mentioned Preston tubes, the two wall static pressure orifices, and the two wall temperature thermocouples are also shown in Fig. 2. The Preston tubes were placed sufficiently far apart so no aerodynamic interference would occur between them and the fence.

The fence operational procedure is relatively simple. It is remotely rotated until the pressure differential between the two orifices becomes zero. At this position the angle is taken as the direction of the local velocity vector which is assumed to correspond to the local surface shear stress vector. The fence is rotated ninety degrees to this position and the two pressures, i.e., forward and aft of the fence are recorded. The corresponding pressure difference $\Delta P_f = P_f - P_b$ is then related to the surface shear stress measured with the balance at the same station and under the same tunnel test conditions.

SECTION III

TEST PROCEDURE

The experiment was conducted in two phases. The surface shear stress measurements with the balance were made during the first phase, while the Preston tubes and boundary layer fence measurements were obtained during the second phase of the experiment. These measurements were made on the upper wall of the M=3 high Reynolds number wind tunnel. The reason for testing on the upper surface rather than the tunnel side wall was to avoid the boundary layer distortion which occurs on the side walls resulting from lateral pressure gradients. All measurements were made at a nominal Mach number of three. The Reynolds number was varied by two methods: (1) by testing at eight different longitudinal stations as shown in Fig. 4, and (2) by changing the stagnation pressure at each tunnel location. This program provided a certain amount of intentional redundancy considered to be necessary because of the difficulty in making accurate surface shear stress measurements with the balance. The combination of test stagnation conditions and wall locations along with the detailed measurements are presented in Table I.

During these tests the stagnation temperature was slightly below the ambient temperature. Under these conditions the unit Reynolds number varied from 10^7 to 10^8 per foot corresponding to a momentum thickness Reynolds number range of 2×10^4 to approximately 54×10^4.

All the data presented is for a wall temperature near the adiabatic temperature and a near zero pressure gradient.

SECTION IV
DATA REDUCTION

A brief description of the data reduction procedure will be presented in this section. The surface shear stress measurements obtained with the floating-element balance were converted to skin friction coefficients by dividing by the dynamic pressure at the edge of the boundary layer, namely:

$$(C_f)_g = \tau_{w_g} / \tfrac{1}{2}\rho_e U_e^2 \tag{1}$$

The corresponding momentum thickness Reynolds number was calculated from the empirical relationship obtained by Fiore,[3] i.e.,

$$R_{e_\theta} = 4.513 \times 10^{-4} M_e^{1.118} R_{e_x}^{0.949} \tag{2}$$

The data used to arrive at eq.(2) was from boundary layer profile measurements made at the same test conditions and location on the tunnel wall as the present investigation.

The Preston tubes were then calibrated for the data and test conditions of this particular experiment. As in the case of Keener and Hopkins[4] it was assumed that the Preston tube calibration is of the form

$$\log\left(\frac{\tau_{w_g} \cdot d^2}{4\rho^* \nu^{*2}}\right) = A_0 \log\left(\frac{\overline{\Delta P}_p \cdot d^2}{4\rho^* \nu^{*2}}\right) + B_0 \tag{3}$$

where the reference density, ρ^*, was calculated from

$$\rho^* = 144 \frac{P_w}{RT^*} \tag{4}$$

In eq. (4) it is assumed that the static pressure through the boundary layer is constant and equal to the wall pressure.

The reference temperature in eq. (4) was calculated from the Sommer and Short expression[6] given as

$$T^* = T_e(0.55 + 0.035\ M_e^2 + 0.45\ \frac{T_w}{T_e}) \tag{5}$$

The reference kinematic viscosity was calculated from the definition

$$\nu^* = \frac{\mu^*}{\rho^*} \tag{6}$$

where Keye's equation for the viscosity was used, namely:

$$\mu^* = 2.32 \times 10^{-8}\ \sqrt{T^*} / \left[1 + \frac{220}{T^*(10^{9/T^*})}\right] \tag{7}$$

In eq.(3) the value of $\overline{\Delta P}_p$ was taken as suggested by Hopkins and Keener[7] rather than the difference between the Preston tube total pressure and the wall static pressure. The purpose for this choice is based on the work of Hopkins and Keener who found that eq.(3) results in a calibration curve for the compressible turbulent boundary layer which would coincide with Preston's equation for the incompressible case[1] of the form

$$\log\left(\frac{\tau_{w_g} \cdot d^2}{4\rho\nu^2}\right) = 0.875\ \log\left(\frac{\Delta P \cdot d^2}{4\rho\nu^2}\right) - 1.396 \tag{8}$$

where $\Delta P = P_{p_t} - P_w$.

The constants A_0 and B_0 in eq.(3) are determined by the least squares fit of the data.

The generalized form of the skin friction coefficient is obtained from eq.(3). This relationship can be shown to be

$$(C_f)_p = 8^{(1\ - A_0\ )}\ .\ 10^{B_0}\ \frac{\left(\frac{M_p}{M_e}\right)^{2A_0}}{\left[\left(\frac{\rho_e}{\rho^*}\right) \times Re_d^{*2}\right]^{(1-A_0)}} \tag{9}$$

where the Preston Mach number, M_p, provided the flow is supersonic, is obtained from iteration of the Rayleigh pitot formula written as

$$\frac{P_{Pt}}{P_w} = \left(\frac{6}{5} M_p^2\right)^{7/2} \left(\frac{1}{\frac{7}{6} M_p^2 - \frac{1}{6}}\right)^{5/2} \tag{10}$$

for γ=1.4.

A similar method must be considered in arriving at an expression for the skin friction coefficient for the boundary layer fence technique. In this investigation it was assumed that the Preston tube diameter, d, in eq.(3) can be replaced with the fence height, h, leading to a fence calibration equation written as

$$\log\left(\frac{\tau_{w_g} \cdot h^2}{4\rho^* \nu^{*2}}\right) = C_0 \log\left(\frac{\Delta P_f \cdot h^2}{4\rho^* \nu^{*2}}\right) + D_0 \tag{11}$$

where $\Delta P_f = P_f - P_b$ and the constants C_0 and D_0 are different than the Preston tube calibration constants. In order to show that these constants must be different, eq.(3) can be re-written as

$$\log\left(\frac{\tau_{w_g} \cdot h^2}{4\rho^* \nu^{*2}}\right) = A_0 \log\left(\frac{\overline{\Delta P}_p \cdot h^2}{4\rho^* \nu^{*2}}\right) + (A_0 - 1)\log\left(\frac{d}{h}\right)^2 + B_0 \tag{12}$$

assuming that

$$\log\left(\frac{\overline{\Delta P}_p \cdot h^2}{4\rho^* \nu^{*2}}\right) = E_0 \log\left(\frac{\Delta P_f \cdot h^2}{4\rho^* \nu^{*2}}\right) + F_0 \tag{13}$$

then eq.(12) becomes

$$\log\left(\frac{\tau_{w_g} \cdot h^2}{4\rho^* \nu^{*2}}\right) = A_0\, E_0 \log\left(\frac{\Delta P_f \cdot h^2}{4\rho^* \nu^{*2}}\right) + \left[A_0\, F_0 + (A_0 - 1)\log\left(\frac{d}{h}\right)^2 + B_0\right] \tag{14}$$

In order for eq.(11) and eq.(14) to be identical, the following must be true

$$C_0 = A_0 E_0 \tag{15}$$

and

$$D_0 = A_0 F_0 + (A_0 - 1) \log \left(\frac{d}{h}\right)^2 + B_0 = f_2\left(\frac{d}{h}\right) \tag{16}$$

From eq.(16) it is noted that the intercept of eq.(11) is a function of the ratio d/h, which is a fictitious parameter, however it does serve to indicate that the calibration constants in eq.(11) are different than those in eq.(3) and must be evaluated separately.

The skin friction coefficient equation for the boundary layer fence is obtained from eq.(11) as

$$(C_f)_f = 8^{(1-C_0)} \cdot 10^{D_0} \frac{\left(\frac{\Delta P_f}{q_e}\right)^{C_0}}{\left[\left(\frac{\rho_e}{\rho^*}\right) R_{e_h}^{*2}\right]^{(1-C_0)}} \tag{17}$$

The experimental measurements were compared with the Van Driest II skin friction theory[8] written in the form

$$(C_f)_{V.D.} = \frac{\left[\sin^{-1}\left(\frac{2A^2 - B}{\sqrt{B^2 + 4A^2}}\right) + \sin^{-1}\left(\frac{B}{\sqrt{B^2 + 4A^2}}\right)\right]^2}{r\left(\frac{\gamma-1}{2}\right) M_e^2 \left[17.08 (\log \overline{R}_{e_\theta})^2 + 25.11 (\log \overline{R}_{e_\theta}) + 6.012\right]} \tag{18}$$

where

$$A = M_e \sqrt{r\left(\frac{\gamma-1}{2}\right)\frac{T_e}{T_w}} \tag{19}$$

$$B = A^2 + \frac{T_e}{T_w} - 1 \tag{20}$$

and

$$\bar{R}_{e_\theta} = \sqrt{\frac{T_e}{T_w}} \left[\frac{1 + \dfrac{220}{T_w \left(10^{9/T_w}\right)}}{1 + \dfrac{220}{T_e \left(10^{9/T_e}\right)}} \right] \times R_{e_\theta} \qquad (21)$$

The data reduced by the method outlined above are presented in Table II.

SECTION V

TEST RESULTS

1. Balance Measurements

In Fig.5 the skin friction coefficient obtained with the floating-element balance in the Reynolds number range $2 \times 10^4 \leq Re_\theta \leq 54 \times 10^4$ is compared with that calculated from the Van Driest theory.[8] Over the complete range of momentum thickness Reynolds number the measured skin friction coefficients are within ±10% of the Van Driest II theory. This agreement between the measurements and theory is considered to be reasonably good. Having established the validity of these measurements, they now can be used to evaluate the skin friction coefficients obtained with the boundary layer fence technique.

2. Preston tube

The Preston tube method was introduced as a second method for obtaining the local skin friction coefficient. The intent was to use the Preston tube results as a separate check on the measurements made with the floating-element balance. In order to accomplish this, it was first necessary to obtain the calibrations constants A_0 and B_0 given in eq.(3).

Figure 6 is a plot of the logarithm of the Preston shear stress parameter, $\tau_{w_g} \cdot d^2/4\rho^* \nu^{*2}$, versus the logarithm of the Preston pressure parameter $\overline{\Delta P}_p \cdot d^2/4\rho^* \nu^{*2}$. The result is a linear function similar to eq.(3). The values of A_0 and B_0 were obtained by the least squares fit to the data and were found to be 0.8677 and -1.3228 respectively. Comparison between the measurements and eq.(3) with the proper constants is presented in Fig. 6. The agreement between the two is excellent. Shown for informational purposes are the calibrations

obtained by Keener and Hopkins[4] as well as Yanta et al.[9] For small values of the Preston pressure parameter, both appear to agree very well with the present measurements and the new calibration. As the Preston pressure parameter is increased the calibration of Keener and Hopkins is in excellent agreement with the present measurements while that of Yanta et al. is somewhat lower than the new measurements. When the new calibration constants are introduced into eq.(9), the Preston skin friction coefficient equation becomes

$$(C_f)_p = 0.0626 \frac{\left(\frac{M_p}{M_e}\right)^{1.7355}}{\left[\left(\frac{\rho_e}{\rho^*}\right) R_{e_d}^{*2}\right]^{0.1323}} \tag{9a}$$

Fig. 7 shows the skin friction coefficient calculated from eq.(9a) plotted versus that obtained with a floating-element balance and Fig. 8 is a plot of $(C_f)_p$ versus the skin friction coefficient calculated from eq.(18). In both cases the Preston tube skin friction coefficients are within ±10% of both the theory and those values obtained with the balance. The Preston tube skin friction coefficient overpredicts the theory at low momentum thickness Reynolds numbers while it underpredicts the theory at higher Reynolds numbers. In both Figs. 7 and 8 the agreement is considered to be within acceptable limits.

3. Boundary Layer Fence

The results of this test indicate that the fence technique is a useful tool for measuring the surface shear stress in a compressible turbulent boundary layer.

As previously mentioned, it is assumed that the fence calibrations should be similar in form to the Preston tube calibration provided the Preston tube outside diameter is replaced with the fence height. This leads to the fence calibration equation given by eq.(11). Fig. 9 is a plot of the logarithm of the fence shear stress parameter, $\tau_{w_g} \cdot h^2/4\rho^* \nu^{*2}$, versus the logarithm of fence pressure parameter, $\Delta P_f \cdot h^2/4\rho^* \nu^{*2}$. Also shown in Fig. 9 is eq.(11) where the calibration constants C_0 and D_0 are 0.9039 and -1.6404 respectively. The agreement between the measurements and eq.(11) is excellent, indicating that eq.(11) with these constants should result in a good expression for the skin friction coefficient as a function of the fence pressure differential, the edge dynamic pressure, the density ratio (ρ_e/ρ^*), and the fence Reynolds number $(R_{e_h}^*)$. This expression is obtained by introducing the above values for C_0 and D_0 into eq.(17), namely:

$$(C_f)_f = 0.028 \frac{\left(\frac{\Delta P_f}{q_e}\right)^{0.9039}}{\left[\left(\frac{\rho_e}{\rho^*}\right) \quad R_{e_h}^{*2}\right]^{0.0962}} \tag{17a}$$

The skin friction coefficient calculated from eq.(17a) is compared with those measured with a balance in Fig. 10 and with the Van Driest II theory in Fig.11. In both cases eq.(17a) gives values which are within ± 10% of both the measurements made with the balance and those calculated from the theory. This agreement is considered to be very good since eq.(17a) is being compared with balance measurements which are no more accurate than ± 10% when compared with theory.

4. Comparison of Techniques

Fig. 12 is a plot of the skin friction coefficient versus the momentum thickness Reynolds number and summarizes the results of this investigation. It contains the skin friction coefficient measurements made directly with the balance, those obtained with the Preston tube, and those taken with the boundary layer fence. Superimposed on Fig. 12 is the Van Driest II theory. The agreement in the skin friction coefficients obtained by the various methods as well as the agreement with theory is considered to be acceptable.

SECTION VI

CONCLUSIONS

An experiment was performed for the purpose of developing the boundary layer fence technique used to measure the surface shear stress in a compressible turbulent boundary layer. Measurements were made at a nominal Mach number of three for momentum thickness Reynolds numbers extending from 2×10^4 to approximately 54×10^4. The results for a near adiabatic wall and zero pressure gradient condition are as follows:

(1) The boundary layer fence is a valid technique for measuring the wall shear stress in a compressible turbulent boundary layer.

(2) The fence calibration equation is a linear logarithmic function similar in form to the Preston tube calibration equation provided the Preston tube outside diameter is replaced with the fence height.

(3) The skin friction coefficients obtained with the fence agree reasonably well with those obtained with a balance. For momentum thickness Reynolds numbers less than 15×10^4 those obtained with the fence were about 10% higher than the Preston tube values and they were in good agreement with the Van Driest II theory. At momentum thickness Reynolds numbers greater than 15×10^4 the fence measurements were 5% to 10% higher than either those obtained with a balance or those calculated from the theory. Since the expressions for the Preston tube and fence skin friction coefficients are dependent on the shear stress measured with the balance, the accuracy of these two methods are similar to the accuracy of the balance measurements which is ± 10% with reference to the Van Driest II theory.

REFERENCES

1. Preston, J.H., "The Determination of Turbulent Skin Friction By Means of Pitot Tubes", ARC-15758 (1954).
2. Fiore, A.W., Moore, D.G., Murray, D.H. and West, J.E., "Design and Calibration of the ARL Mach 3 High Reynolds Number Facility", ARL TR-75-0012 (1975).
3. Fiore, A.W., "M=3 Turbulent Boundary Layer Measurements at Very High Reynolds Numbers", AFFDL TR-77-80 (1978).
4. Keener, E.R. and Hopkins E.J., "Use of Preston Tubes for Measuring Hypersonic Turbulent Skin Friction", NASA TND-5544 (1969).
5. Winter, K.G., "An Outline of the Techniques Available For The Measurement of Skin Friction in Turbulent Boundary Layers", Progress in Aerospace Sciences, Vol.18, No.1 (1977).
6. Sommer, S.C. and Short, Barbara J., "Free-Flight Measurements of Turbulent-Boundary-Layer Skin Friction in the Presence of Severe Aerodynamic Heating at Mach Numbers From 2.8 to 7.0", NACA TN-3391 (1955).
7. Hopkins, E.J. and Keener, E.R., "Comments on 'Calibration of Preston Tubes in Supersonic Flow'", AIAA Journal, Vol.4, No.4 (1966), pp.760-761.
8. Van Driest, E.R., "On Turbulent Flow Near a Wall", J. Aeronaut. Sci., 23, (1956), pp.1007-1011 and 1036.
9. Yanta, W.J., Brott, D.L. and Lee, R.E., "An Experimental Investigation of the Preston Probe Including Effects of Heat Transfer, Compressibility, and Favorable Pressure Gradient", AIAA paper 69-648.
10. Konstantinov, N.I. and Dragnysh, G.L., "Energomashinostroenie", Trudy L.P.I. 176 (1955), pp.191-200.

11. Vagt, J.D. and Fernholz, H., "Use of Surface Fences to Measure Wall Shear Stress in Three-Dimensional Boundary Layers", Aeronaut.Q., XXIV, 2 (1973), pp.87-91.

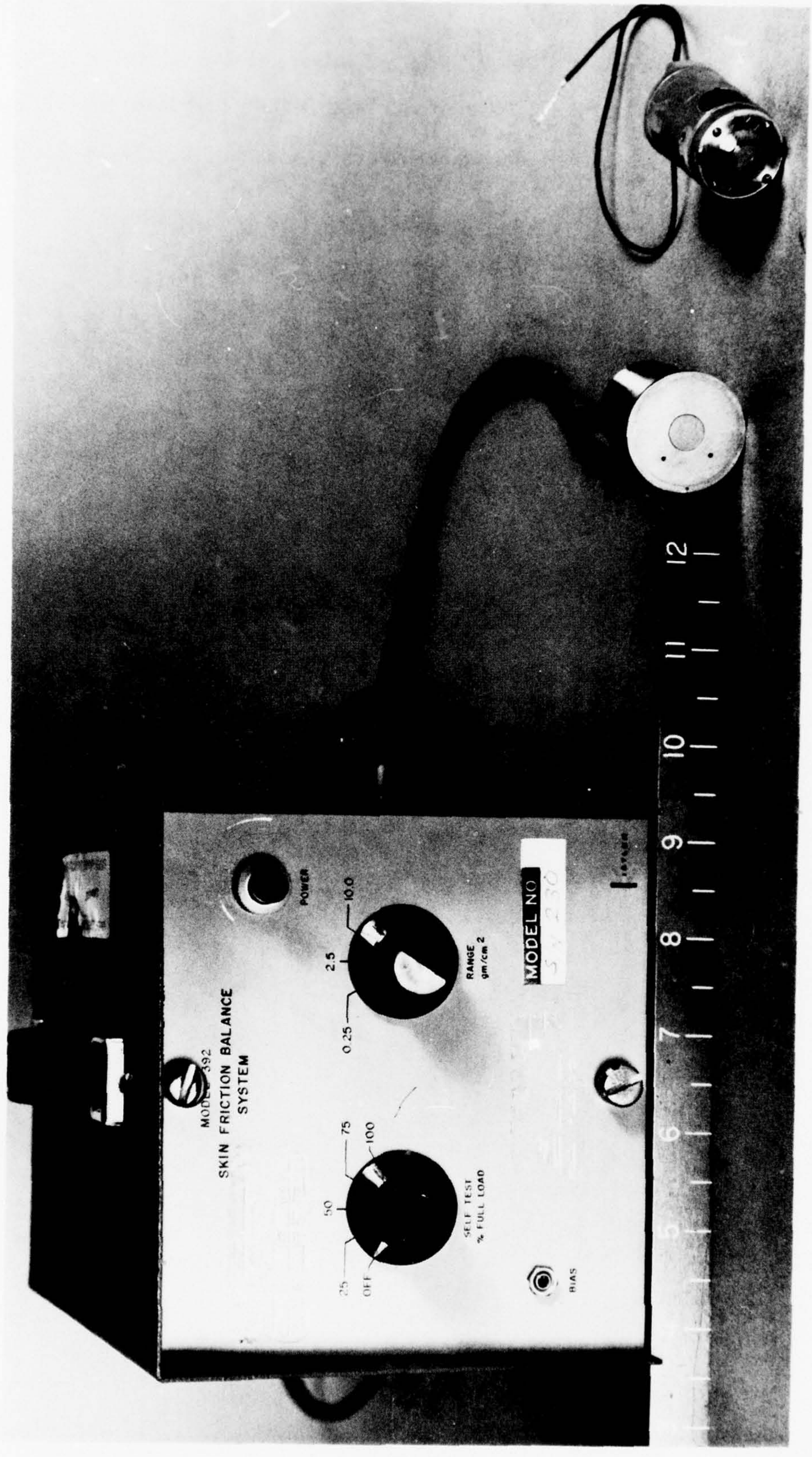

Figure 1. Floating-Element Skin Friction Balance

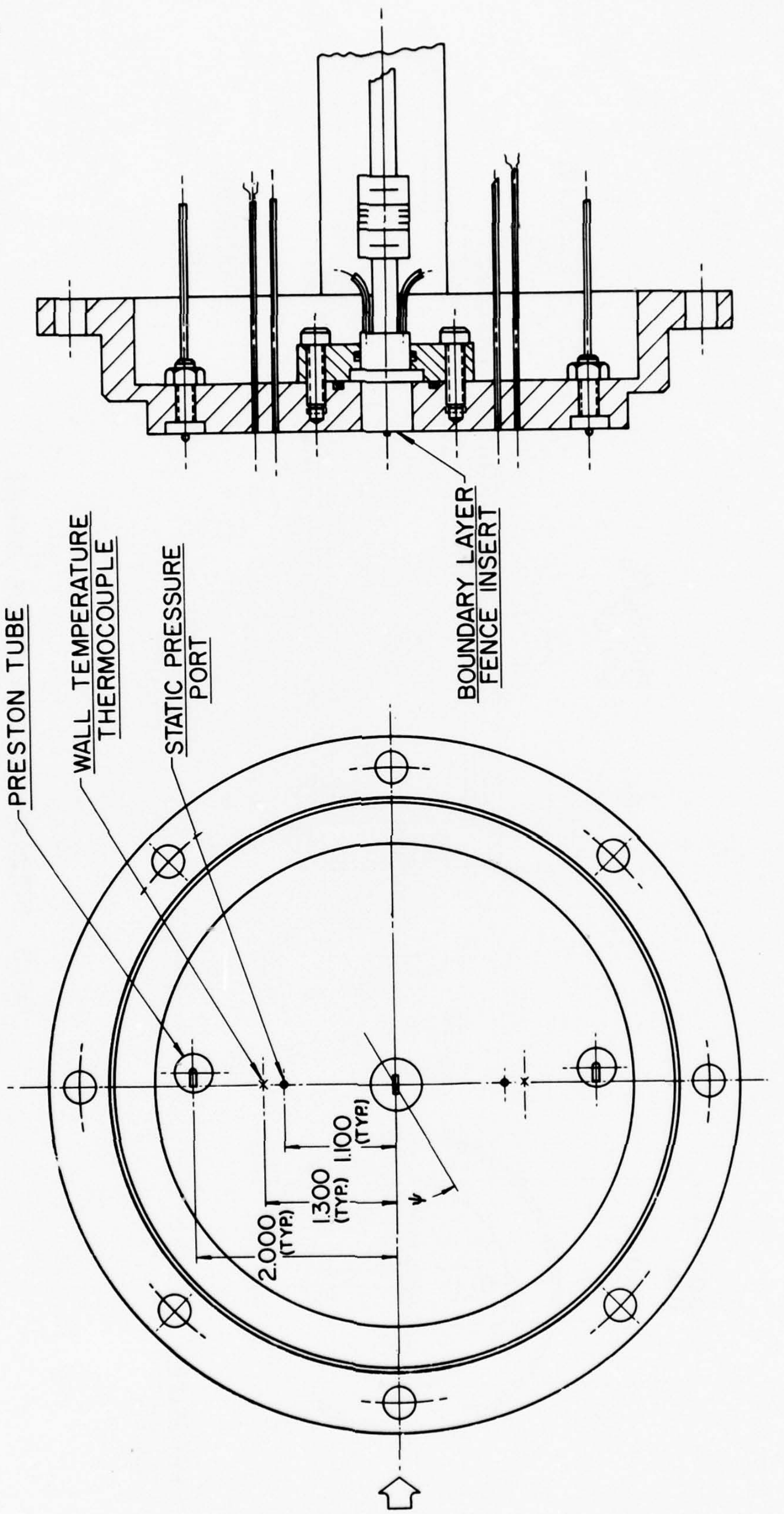

FIG. 2 BOUNDARY LAYER FENCE ASSEMBLY

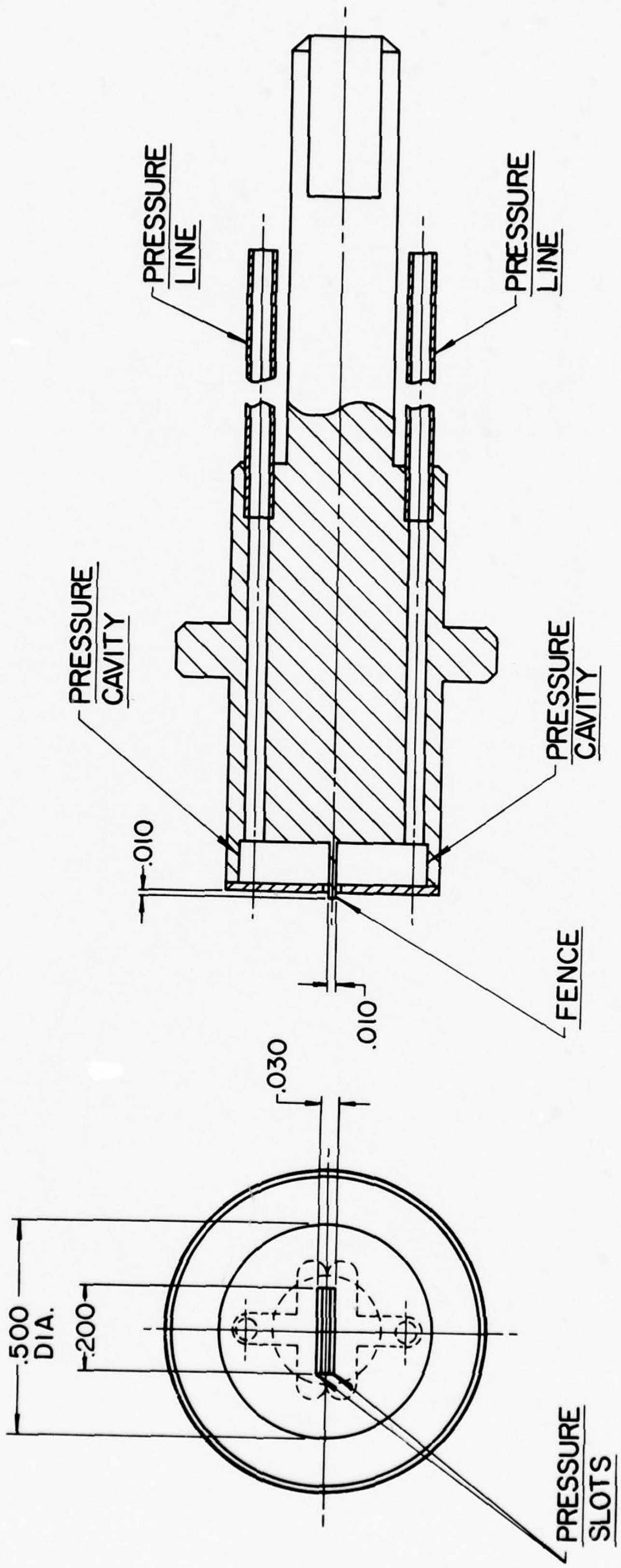

FIG. 3 BOUNDARY LAYER FENCE INSERT

STATION NUMBER	DISTANCE FROM NOZZLE THROAT (INCHES)	STATION NUMBER	DISTANCE FROM NOZZLE THROAT (INCHES)
1	27.28	5	82.28
2	43.28	6	94.28
3	58.28	7	106.28
4	70.28	8	118.28

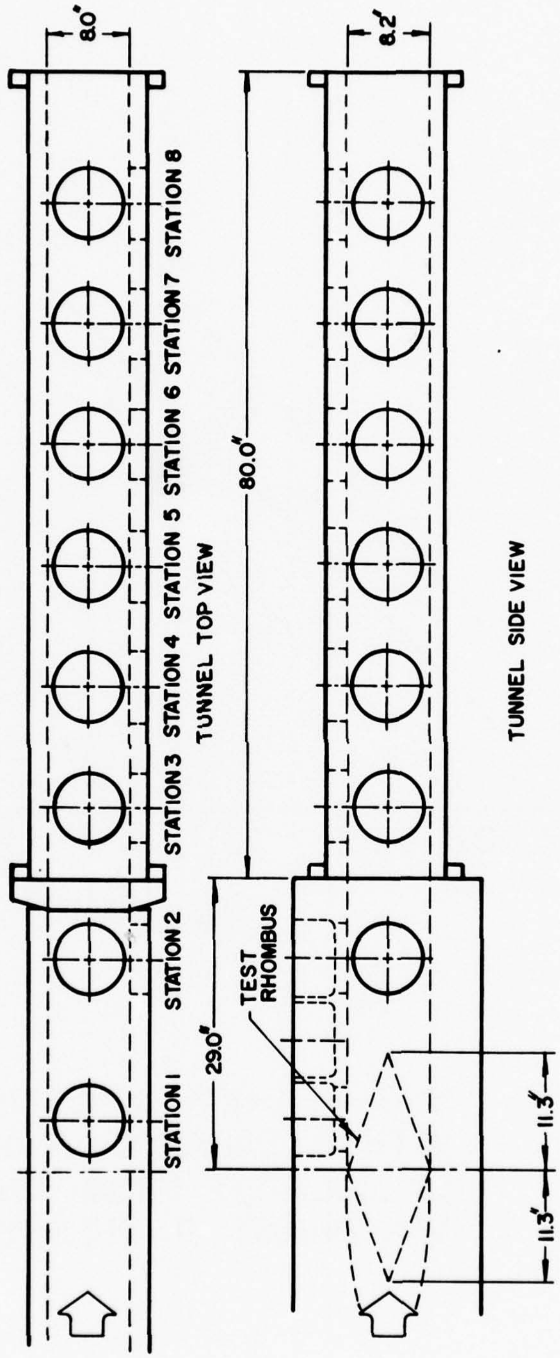

FIG. 4 SCHEMATIC OF TUNNEL TEST SECTION AND DIFFUSER SECTION

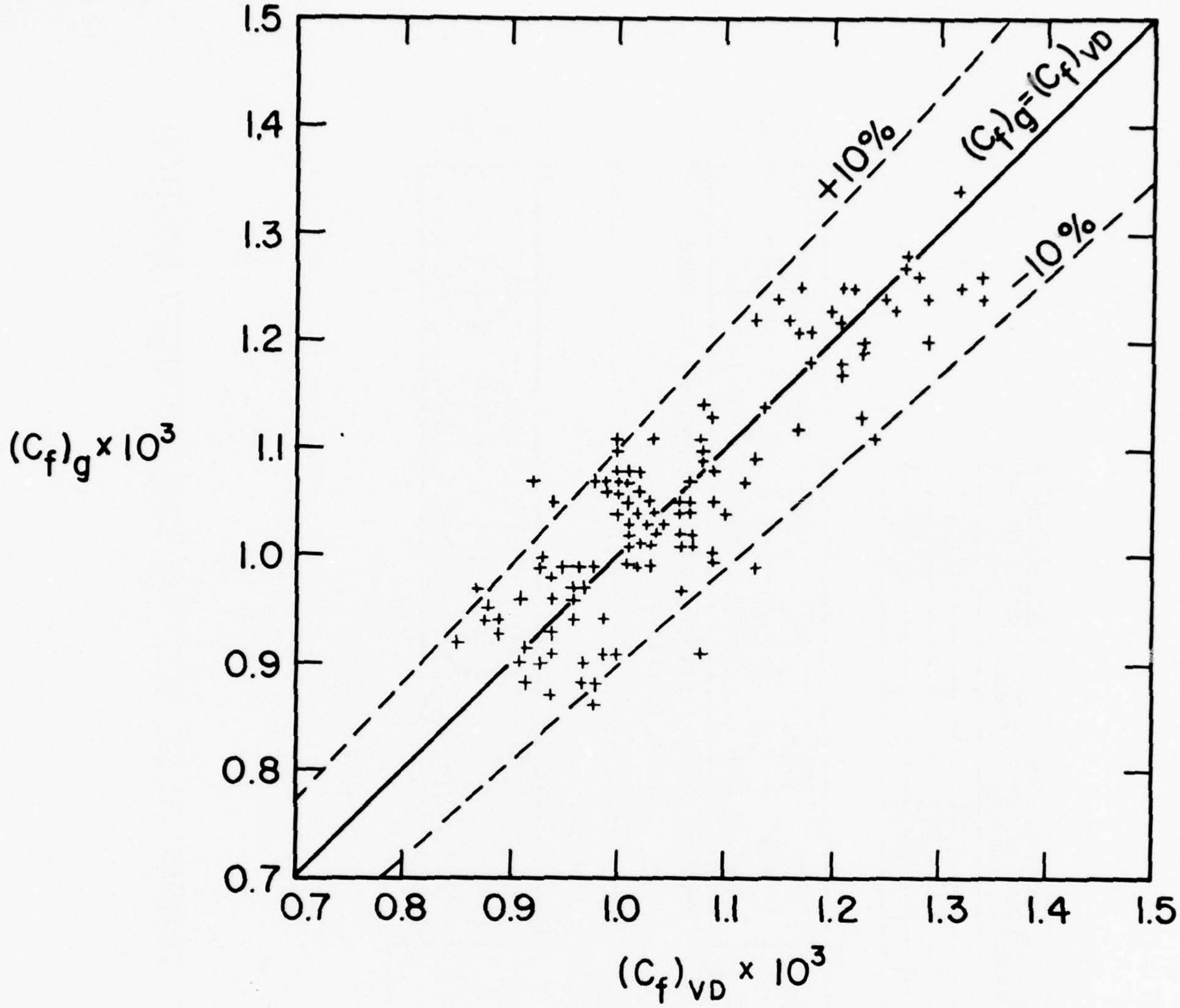

FIG. 5 SKIN FRICTION COEFFICIENT OBTAINED WITH A BALANCE VERSUS THAT CALCULATED FROM THE VAN DRIEST II THEORY.

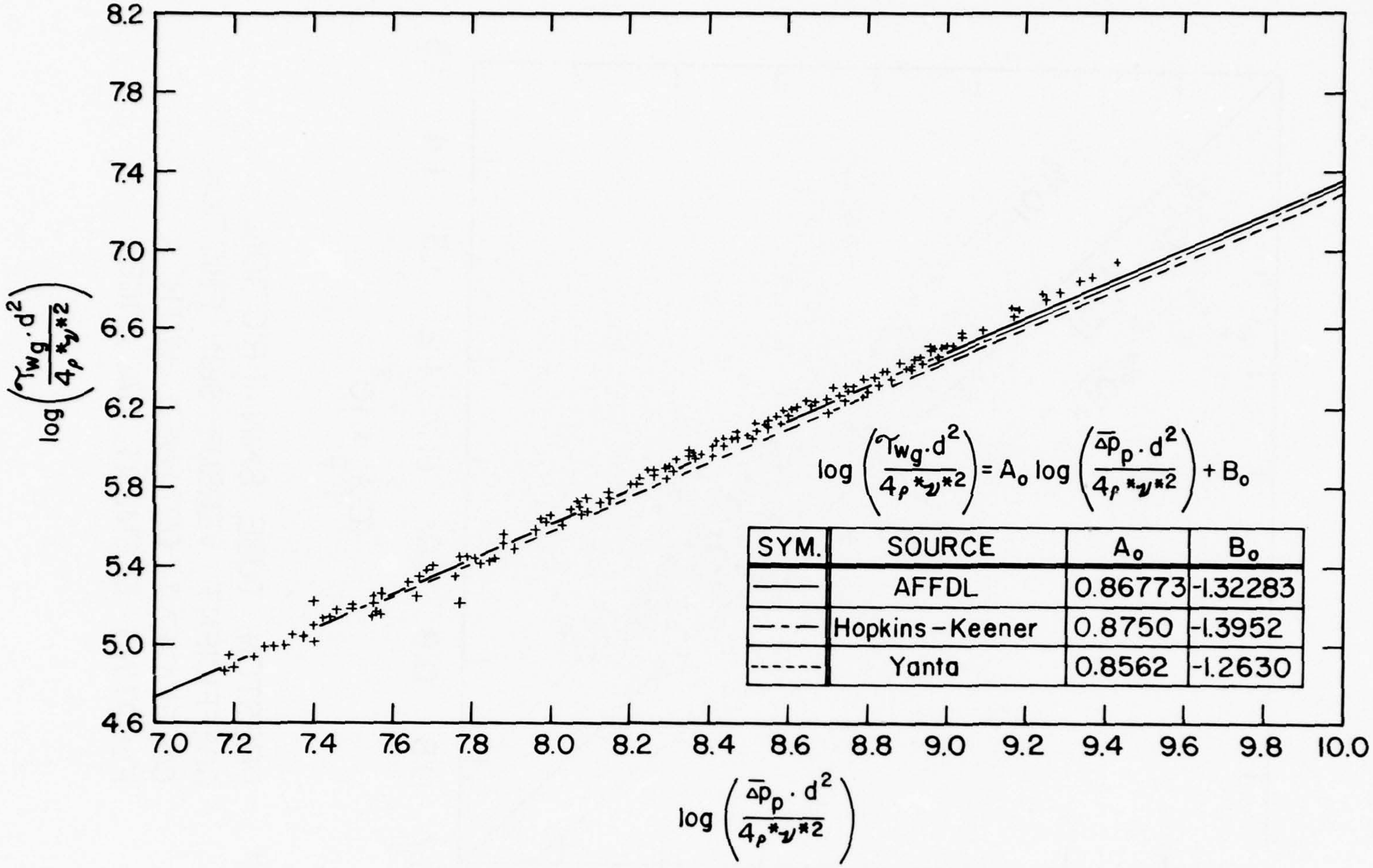

FIG. 6 THE MEASURED SHEAR STRESS PARAMETER VERSUS THE PRESTON TUBE PARAMETER FOR $M_e = 2.86$ AND $2 \times 10^4 \leq R_{e_\theta} \leq 54 \times 10^4$

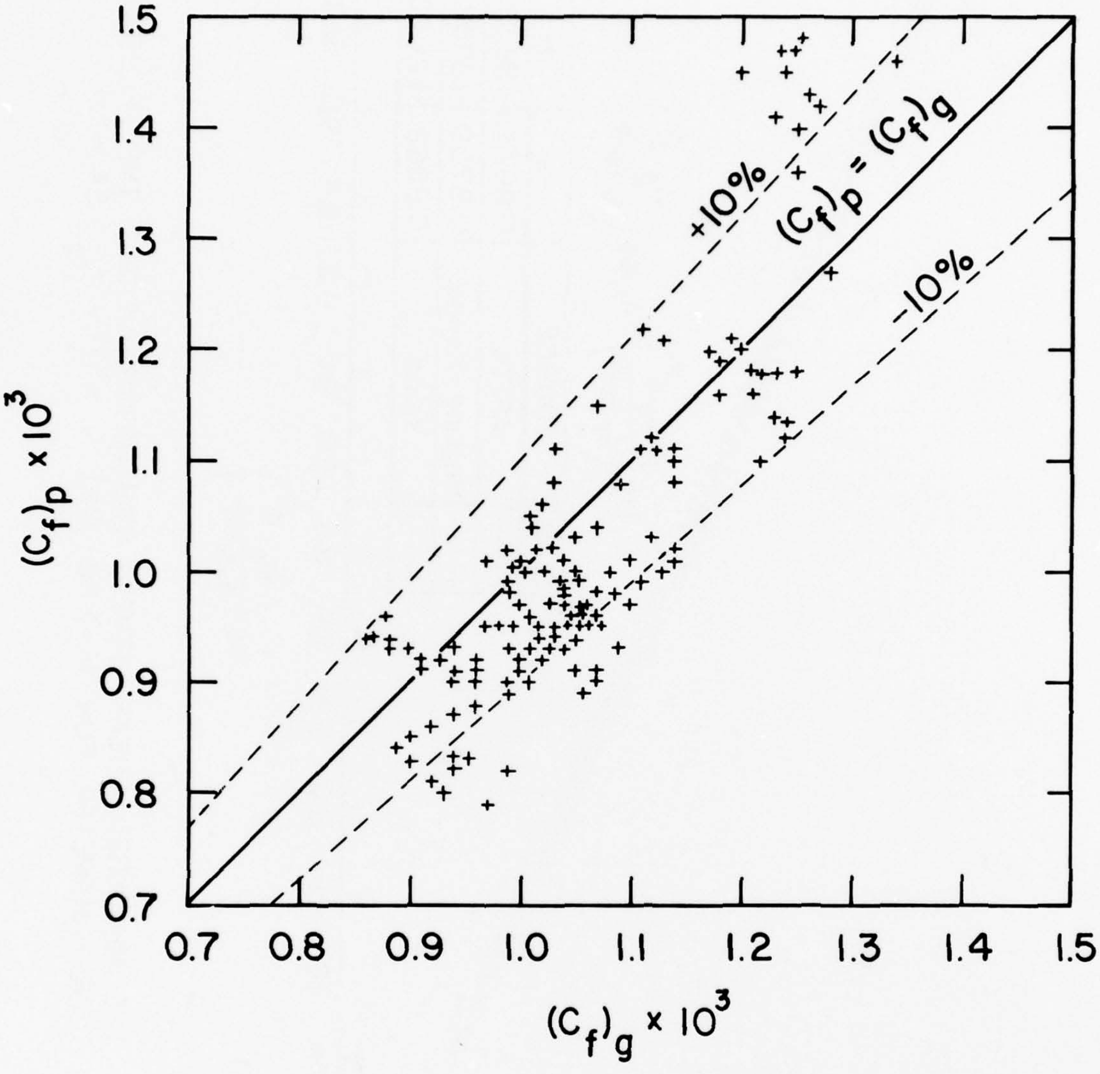

FIG. 7 PRESTON TUBE SKIN FRICTION COEFFICIENT VERSUS SKIN FRICTION COEFFICIENT OBTAINED WITH A FLOATING-ELEMENT BALANCE.

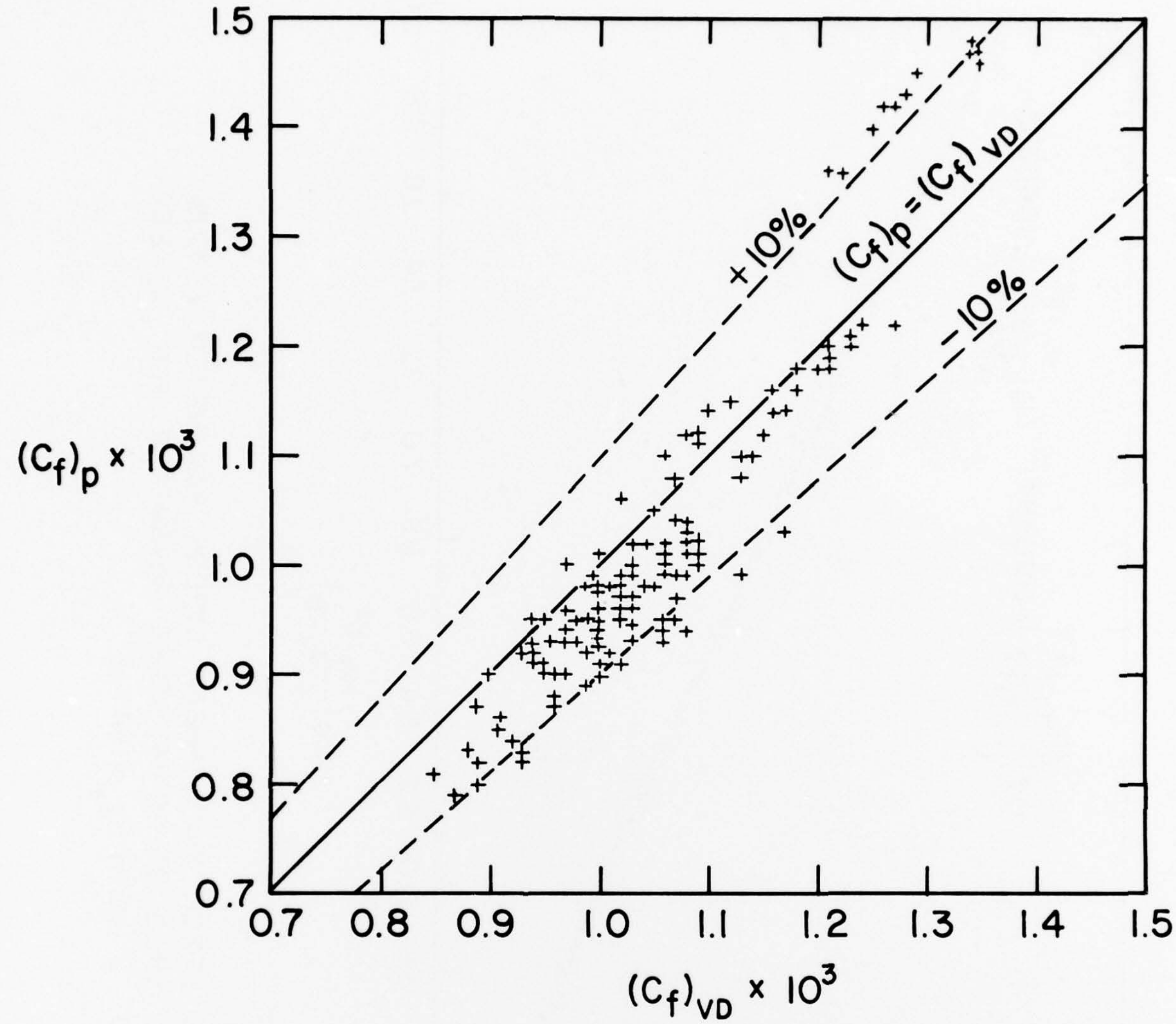

FIG. 8 PRESTON TUBE SKIN FRICTION COEFFICIENT VERSUS THAT CALCULATED FROM THE VAN DRIEST II THEORY.

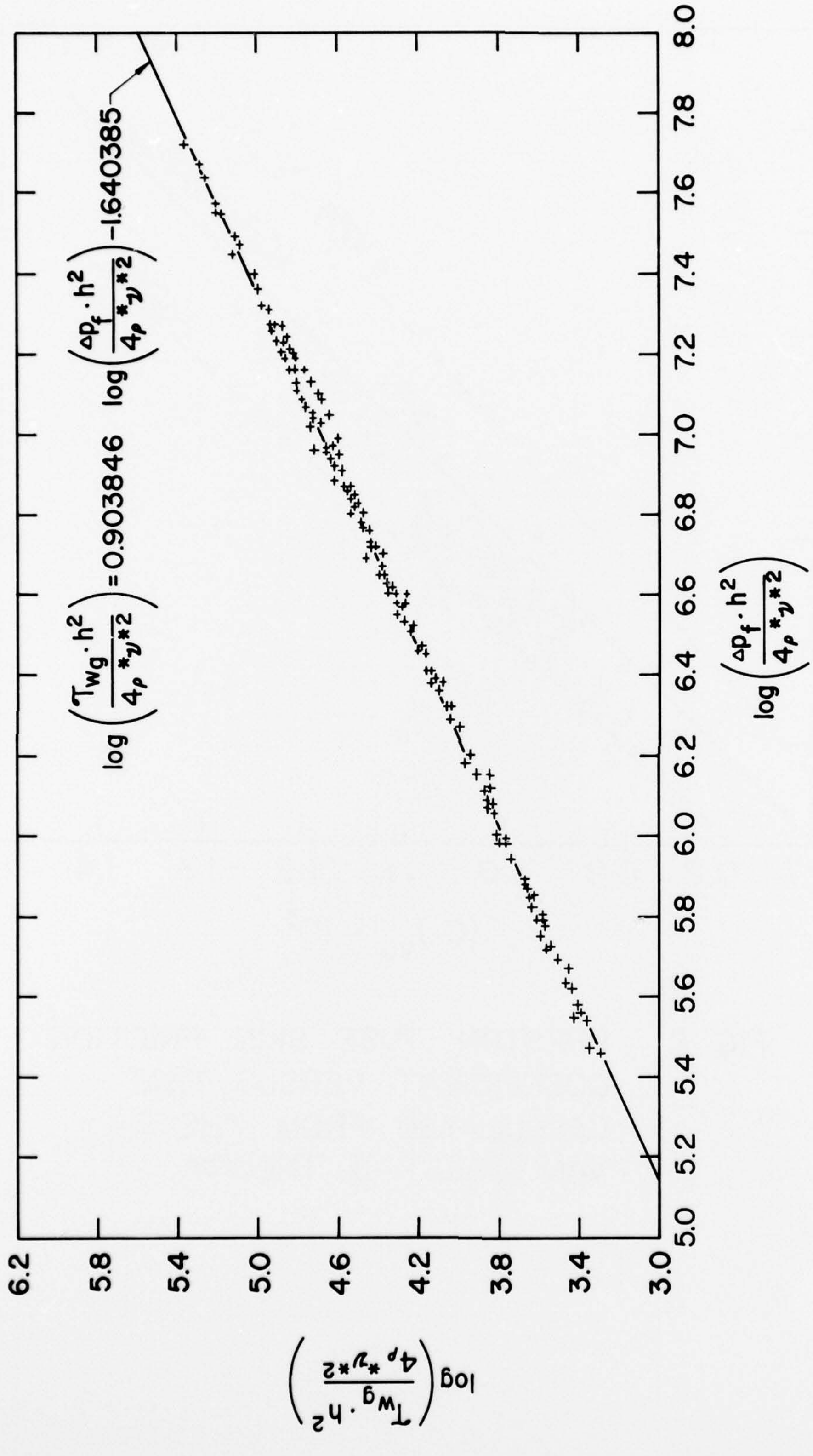

FIG. 9 THE FENCE WALL SHEAR STRESS PARAMETER VERSUS THE WALL STATIC PRESSURE PARAMETER FOR $M_e = 2.86$ AND $2 \times 10^4 \leq R_{e_\theta} \leq 54 \times 10^4$.

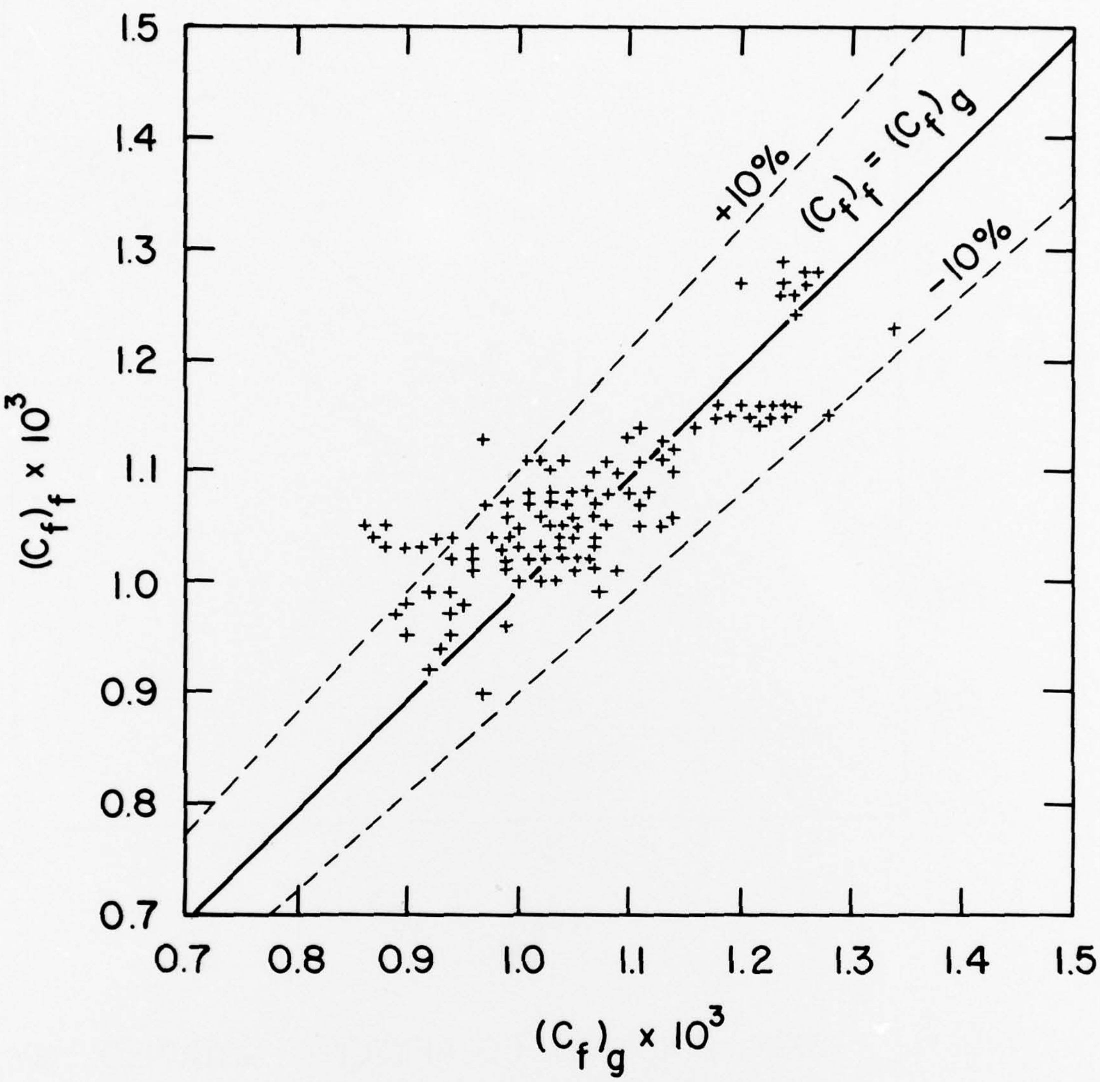

FIG. 10 BOUNDARY LAYER FENCE SKIN FRICTION COEFFICIENT VERSUS SKIN FRICTION COEFFICIENT OBTAINED WITH A FLOATING-ELEMENT BALANCE.

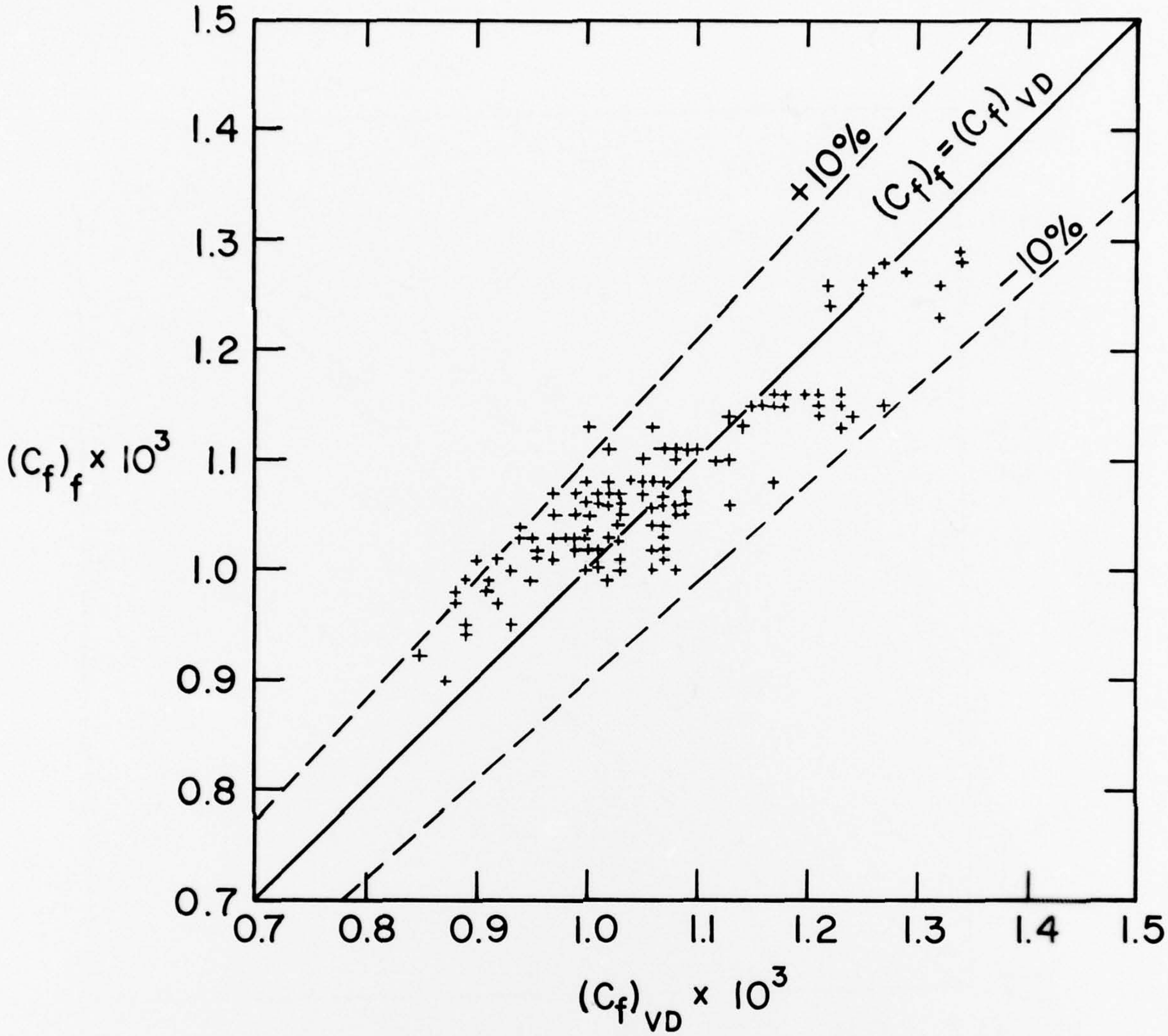

FIG. 11 SKIN FRICTION COEFFICIENT OBTAINED BY THE FENCE METHOD VERSUS THE VAN DRIEST II THEORY.

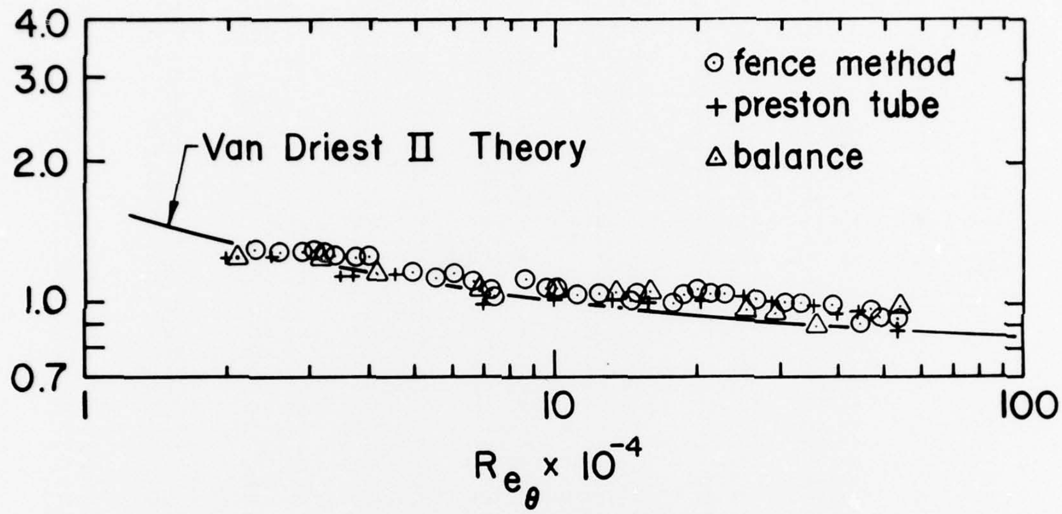

FIG. 12 SKIN FRICTION COEFFICIENT VERSUS MOMENTUM THICKNESS REYNOLDS NUMBER FOR $M_e = 2.86$, NEAR ADIABATIC WALL AND ZERO PRESSURE GRADIENT CONDITIONS.

TABLE 1

RECORDED MEASUREMENTS

TEST NO.	STA. NO.	X INCHES	P_0 PSIA	T_0 DEG R	P_W PSIA	T_W DEG R	P_{P_T} PSIA	P_F PSIA	P_B PSIA	TAU_{W_G} LBS/FT**2
1	1	27.28	75.23	472.82	2.130	497.905	8.025	3.61	1.18	2.5491
2	1	27.28	79.08	471.99	2.195	481.460	8.520	3.83	1.22	2.4577
3	1	27.28	93.18	470.80	2.550	468.995	10.285	4.59	1.39	2.7621
4	1	27.28	101.81	477.90	2.785	461.965	11.480	5.06	1.49	3.1231
5	1	27.28	112.38	477.15	3.060	456.085	12.870	5.64	1.62	3.4889
6	1	27.28	124.86	476.68	3.370	449.465	14.480	6.30	1.76	3.7876
7	1	27.28	130.68	474.41	3.510	443.845	15.115	6.61	1.83	3.9804
8	1	27.28	147.54	469.20	4.005	445.525	17.310	7.54	2.05	4.5449
9	1	27.28	86.34	466.94	2.360	441.565	9.610	4.31	1.30	2.6397
10	1	27.28	115.20	466.05	3.115	436.120	13.255	5.87	1.66	3.6056
11	1	27.28	85.73	464.52	2.335	433.110	9.595	4.27	1.30	2.6612
12	1	27.28	151.86	463.87	4.055	425.575	17.950	7.83	2.08	4.6505
13	2	44.68	161.16	474.30	5.640	473.600	18.650	9.12	2.84	4.9663
14	2	44.68	225.59	466.68	7.840	436.130	27.360	13.06	3.79	6.3429
15	2	44.68	234.90	459.76	8.170	420.200	28.480	13.60	3.94	6.6564
16	2	44.68	240.72	456.15	8.370	412.430	29.450	13.97	4.01	7.7092
17	2	44.68	242.04	464.41	8.475	453.135	29.605	13.66	3.90	7.1488
18	2	44.68	266.16	458.12	9.340	422.765	33.115	15.23	4.22	7.8643
19	2	44.68	286.26	447.45	10.050	396.535	35.865	16.41	4.40	8.3848
20	2	44.68	306.41	441.37	10.760	381.275	38.980	17.78	4.72	8.8889
21	2	44.68	324.77	437.75	11.415	372.130	41.325	18.98	4.98	9.4438
22	2	44.68	344.58	478.58	11.750	448.380	42.740	19.58	5.02	9.9391
23	2	44.68	365.16	468.91	12.480	421.030	46.020	20.90	5.37	10.7240
24	2	44.68	383.27	461.05	13.140	404.970	48.870	22.14	5.62	11.0569
25	2	44.68	421.68	452.56	14.490	388.810	54.720	24.70	6.19	12.7046
26	2	44.68	164.27	446.11	5.880	391.760	19.530	9.40	2.73	5.2650
27	2	44.68	217.38	446.90	7.700	388.860	26.400	12.53	3.46	6.1627
28	2	44.68	228.66	476.24	7.940	474.440	27.220	12.86	3.66	6.5495
29	2	44.68	237.84	474.23	8.290	450.220	28.715	13.53	3.76	7.6617
30	2	44.68	239.81	470.84	8.385	437.235	28.970	13.73	3.77	7.1157
31	2	44.68	263.40	468.84	9.205	426.910	32.305	15.13	4.12	7.8090
32	2	44.68	284.34	461.52	9.940	415.380	35.160	16.47	4.40	8.4758
33	2	44.68	301.80	457.35	10.575	406.775	37.725	17.52	4.62	9.0076
34	2	44.68	322.02	452.70	11.275	395.465	40.495	18.85	4.89	9.5814
35	2	44.68	344.04	489.42	11.510	472.925	42.470	19.58	5.08	10.2487
36	2	44.68	358.86	482.08	12.015	447.480	45.010	20.55	5.29	10.6022
37	2	44.68	379.26	473.04	12.730	427.715	47.650	21.94	5.53	11.2058
38	3	59.68	65.88	478.80	2.140	508.960	6.320	3.26	1.20	2.0197
39	3	59.68	73.13	477.83	2.365	493.515	7.150	3.66	1.29	2.3121
40	3	59.68	84.18	483.98	2.710	483.800	8.365	4.26	1.44	2.7555
41	3	59.68	91.38	482.44	2.930	475.790	9.150	4.66	1.53	2.9888
42	3	59.68	63.18	476.28	2.055	473.280	6.150	3.13	1.13	1.9082
43	3	59.68	68.58	475.77	2.225	470.200	6.715	3.44	1.21	2.2166
44	3	59.68	77.63	474.91	2.500	464.400	7.685	3.93	1.34	2.4800
45	3	59.68	79.38	474.23	2.550	461.125	7.890	4.03	1.36	2.6444
46	3	59.68	90.30	473.76	2.895	457.160	9.105	4.63	1.51	2.8836
47	3	59.68	60.54	472.86	1.975	456.780	5.870	3.02	1.08	2.1070
48	3	59.68	71.63	472.28	2.310	454.975	7.070	3.62	1.24	2.3324
49	3	59.68	80.76	471.49	2.595	452.420	8.100	4.12	1.38	2.7377
50	3	59.68	102.72	471.20	3.275	447.270	10.525	5.32	1.67	3.3988

TABLE I (CONT.)

RECORDED MEASUREMENTS

TEST NO.	STA. NO.	X INCHES	P_0 PSIA	T_0 DEG R	P_W PSIA	T_W DEG R	P_{P_T} PSIA	P_F PSIA	P_B PSIA	TAU_{W_G} LBS/FT**2
51	3	59.68	111.90	470.77	3.565	442.965	11.535	5.84	1.80	2.0925
52	3	59.68	124.80	470.20	3.970	439.670	13.015	6.54	1.97	4.1021
53	3	59.68	81.23	467.96	2.620	438.835	8.190	4.17	1.38	2.6931
54	3	59.68	101.58	468.94	3.245	435.950	10.400	5.28	1.65	3.4021
55	4	71.68	306.41	481.32	9.815	440.615	35.270	16.78	4.36	7.2926
56	4	71.68	321.12	477.80	10.280	427.090	37.350	17.59	4.54	8.5803
57	4	71.68	323.04	474.26	10.340	419.525	37.330	17.83	4.55	7.5192
58	4	71.68	343.13	469.35	10.980	410.915	39.995	18.97	4.80	8.2907
59	4	71.68	361.55	487.38	11.530	463.675	41.595	19.85	5.09	8.4298
60	4	71.68	383.34	483.23	12.225	442.660	44.465	21.32	5.35	9.5988
61	4	71.68	398.22	474.76	12.686	427.210	46.765	22.32	5.51	11.2935
62	4	71.68	402.00	466.90	12.815	410.520	47.125	22.62	5.54	10.3699
63	4	71.68	427.32	468.70	13.545	449.635	49.800	23.70	6.02	10.9544
64	4	71.68	125.04	458.89	4.000	463.220	13.035	6.53	2.02	3.2649
65	4	71.68	157.91	453.29	5.055	455.910	16.865	8.35	2.46	4.3433
66	4	71.68	236.94	454.98	7.565	431.405	26.485	12.84	3.48	6.3445
67	4	71.68	297.30	453.26	9.480	410.920	33.900	16.37	4.25	7.0553
68	4	71.68	317.52	454.87	10.150	395.190	36.650	17.52	4.51	7.5262
69	4	71.68	337.38	459.40	10.790	382.230	39.510	18.72	4.76	8.2856
70	4	71.68	357.90	466.79	11.420	369.005	42.095	20.06	5.01	8.8069
71	4	71.68	160.13	434.38	5.160	370.860	17.765	8.66	2.41	4.3714
72	4	71.68	238.73	474.26	7.610	481.155	26.395	12.73	3.55	6.2603
73	4	71.68	319.50	467.85	10.160	448.030	36.475	17.38	4.58	8.4291
74	4	71.68	381.84	466.57	12.120	423.140	44.490	21.23	5.33	9.3643
75	4	71.68	396.48	462.18	12.595	402.000	46.870	22.22	5.51	9.9725
76	5	83.68	152.45	455.74	5.300	474.535	16.145	8.41	2.66	4.5445
77	5	83.68	159.77	450.48	5.545	446.595	17.230	8.89	2.75	4.8532
78	5	83.68	168.90	447.64	5.855	433.755	18.415	9.44	2.88	5.0916
79	5	83.68	180.18	447.45	6.240	420.760	19.815	10.19	3.02	5.3691
80	5	83.68	189.05	445.66	6.545	412.405	20.915	10.69	3.15	5.6396
81	5	83.68	198.41	441.63	6.860	398.755	22.110	11.32	3.26	5.7833
82	5	83.68	218.45	439.88	7.530	388.265	24.680	12.52	3.55	6.3829
83	5	83.68	79.38	438.05	2.785	420.705	8.145	4.33	1.50	2.5552
84	5	83.68	125.45	441.44	4.345	407.065	13.420	7.02	2.16	3.9242
85	5	83.68	132.77	444.84	4.600	400.700	14.385	7.41	2.30	4.2789
86	5	83.68	143.40	455.26	4.975	483.860	15.080	7.85	2.54	4.4571
87	5	83.68	153.54	447.53	5.320	456.610	16.345	8.49	2.67	4.8153
88	5	83.68	173.27	443.88	5.990	431.980	18.870	9.68	2.94	5.3604
89	5	83.68	180.41	439.20	6.230	417.830	19.785	10.14	3.03	5.4353
90	5	83.68	191.40	435.32	6.620	403.610	21.350	10.82	3.18	5.6455
91	5	83.68	200.52	432.30	6.930	392.730	22.560	11.41	3.30	5.9454
92	5	83.68	209.81	429.34	7.240	382.960	23.800	11.96	3.44	6.0582
93	5	83.68	219.48	427.07	7.565	375.810	24.920	12.58	3.56	6.4963
94	5	83.68	228.23	424.27	7.870	366.750	26.145	13.09	3.70	6.7497
95	5	83.68	259.50	423.02	8.930	359.380	29.950	14.94	4.16	7.7430
96	6	95.68	66.05	460.87	2.265	483.630	6.425	3.38	1.28	1.9872
97	6	95.68	73.44	456.84	2.500	469.790	7.230	3.80	1.38	2.1286
98	6	95.68	82.62	454.79	2.795	459.780	8.265	4.31	1.53	2.6035
99	6	95.68	86.27	454.32	2.910	452.140	8.670	4.52	1.58	2.5961
100	6	95.68	93.59	454.50	3.145	445.510	9.595	4.96	1.68	2.9588

TABLE I (CONT.)

RECORDED MEASUREMENTS

TEST NO.	STA. NO.	X INCHES	P 0 PSIA	T 0 DEG R	P W PSIA	T W DEG R	P P T PSIA	P F PSIA	P B PSIA	TAU W G LBS/FT**2
101	6	95.68	106.55	452.70	3.565	436.800	11.005	5.68	1.88	3.3575
102	7	107.68	108.36	456.80	4.025	455.160	11.800	6.16	2.06	3.2009
103	7	107.68	122.94	453.95	4.545	435.520	13.500	7.09	2.30	3.6857
104	7	107.68	135.72	449.85	5.025	427.070	15.375	7.77	2.51	3.9243
105	7	107.68	143.04	447.20	5.290	414.360	16.230	8.22	2.62	4.2418
106	7	107.68	151.91	445.55	5.605	406.600	17.395	8.80	2.73	4.4783
107	7	107.68	155.70	443.80	5.740	400.570	17.890	9.03	2.80	5.0328
108	7	107.68	163.26	442.56	6.010	395.270	18.860	9.44	2.97	4.6992
109	7	107.68	172.50	440.88	6.335	388.750	19.930	10.18	3.05	5.0077
110	7	107.68	181.62	449.60	6.690	466.945	20.240	10.39	3.33	5.2567
111	7	107.68	193.02	442.34	7.085	435.815	22.020	11.10	3.48	5.4118
112	7	107.68	202.02	437.67	7.410	418.360	23.210	11.74	3.60	5.7790
113	7	107.68	211.08	433.90	7.725	406.310	24.410	12.38	3.71	5.8604
114	7	107.68	222.30	429.27	8.130	391.760	25.935	13.14	3.87	6.2026
115	7	107.68	231.41	426.21	8.460	381.830	27.120	13.73	4.01	6.3214
116	7	107.68	236.76	422.10	8.655	370.200	28.040	14.07	4.08	7.3399
117	7	107.68	240.72	419.20	8.800	362.675	28.655	14.35	4.12	6.9160
118	7	107.68	262.91	417.99	9.590	354.725	31.510	15.86	4.45	7.3422
119	7	107.68	282.54	415.52	10.290	347.430	34.345	16.95	4.78	7.7212
120	7	107.68	301.26	442.04	10.920	438.400	34.985	17.82	5.26	8.1469
121	7	107.68	321.54	436.03	11.630	406.340	38.140	19.23	5.57	8.5048
122	7	107.68	341.76	431.29	12.370	387.635	41.080	20.60	5.88	8.8440
123	7	107.68	361.86	424.88	13.100	367.425	44.110	21.99	6.15	9.2717
124	7	107.68	381.84	426.21	13.815	352.705	46.995	23.16	6.51	9.8776
125	7	107.68	398.45	420.31	14.400	339.230	49.445	24.47	6.72	11.4013
126	7	107.68	422.09	469.42	15.180	440.060	50.250	25.58	7.15	11.4804
127	7	107.68	440.58	447.01	15.855	404.565	54.250	26.85	7.33	11.8916
128	7	107.68	458.76	447.72	16.545	386.690	57.085	27.86	7.63	12.3613
129	7	107.68	478.91	433.01	17.295	367.085	59.855	29.20	7.90	12.8283
130	7	107.68	498.66	437.48	18.015	368.425	63.185	30.59	8.16	13.3412
131	7	107.68	520.14	453.88	18.660	423.920	64.540	31.13	8.86	13.7605
132	7	107.68	549.90	443.80	19.885	381.465	69.835	33.12	9.12	15.3302
133	8	119.68	82.62	449.38	3.100	452.355	8.415	4.64	1.73	2.5976
134	8	119.68	91.73	453.00	3.410	437.585	9.530	5.16	1.86	2.8100
135	8	119.68	102.72	450.91	3.775	427.660	10.670	5.80	2.01	3.1325
136	8	119.68	113.70	459.66	4.150	417.830	11.945	6.41	2.16	3.3323
137	8	119.68	124.73	451.50	4.515	409.030	13.220	7.08	2.30	3.6887
138	8	119.68	135.59	462.03	4.885	401.570	14.570	7.67	2.48	4.0729
139	8	119.68	144.12	451.02	5.170	395.605	15.660	8.18	2.58	4.2657
140	8	119.68	155.70	453.44	5.600	401.305	17.050	8.72	2.81	4.5030
141	8	119.68	161.34	453.37	5.785	340.365	17.775	9.06	2.89	5.0312
142	8	119.68	163.26	448.87	5.855	384.025	18.040	9.17	2.92	4.7568
143	8	119.68	172.44	449.56	6.190	378.710	19.210	9.75	3.05	5.0585
144	8	119.68	183.36	440.70	6.555	372.655	20.425	10.41	3.16	5.3291
145	8	119.68	192.23	448.31	6.860	368.005	21.525	10.93	3.29	5.5869
146	8	119.68	203.52	454.17	7.250	363.530	22.940	11.54	3.48	5.8283
147	8	119.68	212.76	453.26	7.570	359.200	24.070	12.12	3.59	6.1335
148	8	119.68	220.02	447.23	7.820	355.090	24.885	12.55	3.71	6.3452
149	8	119.68	231.12	448.46	8.195	350.660	26.425	13.21	3.87	6.5519

TABLE II

CALCULATED RESULTS

TEST NO.	MP ME	DELTA_PF QE	RHO_E RHO*	R*ED * 10 ** -4	R*EH * 10 ** -4	LOG F3	LOG F4	LOG F5
1	.5349	.1843	2.1715	1.6580	.2674	5.0007	7.3294	3.4159
2	.5419	.1904	2.1404	1.7800	.2871	5.0233	7.3961	3.4385
3	.5524	.1997	2.1174	2.1349	.3443	5.1594	7.5660	3.5746
4	.5594	.2039	2.0806	2.3610	.3808	5.2543	7.6567	3.6695
5	.5653	.2085	2.0693	2.6334	.4247	5.3531	7.7584	3.7683
6	.5712	.2130	2.0573	2.9512	.4760	5.4416	7.8638	3.8568
7	.5713	.2149	2.0503	3.1225	.5036	5.4920	7.9115	3.9072
8	.5738	.2173	2.0629	3.5526	.5730	5.6091	8.0301	4.0243
9	.5553	.2028	2.0545	2.1141	.3410	5.1516	7.5490	3.5668
10	.5682	.2139	2.0473	2.8345	.4572	5.4176	7.8221	3.8328
11	.5578	.2019	2.0394	2.1401	.3452	5.1665	7.5603	3.5817
12	.5796	.2232	2.0301	3.8018	.6132	5.4176	7.8458	3.8328
13	.5193	.1981	2.0020	4.4607	.7195	5.7337	8.1280	4.1489
14	.5354	.2097	1.9301	6.8099	1.0984	6.0472	8.5063	4.4624
15	.5393	.2097	1.9056	7.4121	1.1955	6.1183	8.5805	4.5335
16	.5383	.2110	1.8943	7.7626	1.2520	6.2091	8.6165	4.6243
17	.5369	.2049	1.9751	7.0683	1.1400	6.1091	8.5510	4.5243
18	.5419	.2100	1.9122	8.4143	1.3571	6.2462	8.6950	4.6614
19	.5454	.2139	1.8648	9.7328	1.5698	6.3598	8.8175	4.7750
20	.5490	.2163	1.8427	10.9221	1.7616	6.4484	8.9181	4.8636
21	.5489	.2186	1.8262	11.9105	1.9210	6.5207	8.9894	4.9359
22	.5466	.2178	1.9414	9.8745	1.5927	6.3906	8.8494	4.8058
23	.5513	.2190	1.8943	11.2670	1.8173	6.4992	8.9609	4.9144
24	.5545	.2215	1.8699	12.4104	2.0017	6.5690	9.0442	4.9842
25	.5598	.2253	1.8463	14.3535	2.3151	6.7082	9.1733	5.1234
26	.5235	.2039	1.8513	5.7613	.9292	5.9338	8.3233	4.3490
27	.5323	.2107	1.8464	7.6138	1.2280	6.1240	8.5789	4.5392
28	.5298	.2054	2.0030	6.2703	1.0113	5.9998	8.4415	4.4150
29	.5336	.2093	1.9463	6.9263	1.1171	6.1238	8.5216	4.5390
30	.5332	.2112	1.9205	7.2362	1.1671	6.1197	8.5532	4.5349
31	.5381	.2126	1.8996	8.1564	1.3155	6.2186	8.6604	4.6338
32	.5407	.2159	1.8870	9.1070	1.4689	6.3138	8.7574	4.7290
33	.5437	.2171	1.8736	9.9262	1.6010	6.3855	8.8340	4.8007
34	.5458	.2203	1.8553	10.9347	1.7637	6.4641	8.9171	4.8793
35	.5489	.2195	1.9848	9.1163	1.4704	6.3467	8.7933	4.7619
36	.5538	.2213	1.9393	10.1319	1.6342	6.4245	8.8827	4.8397
37	.5539	.2249	1.9097	11.3143	1.8249	6.5131	8.9720	4.9285
38	.4761	.1655	2.1145	1.5823	.2552	4.8725	7.1761	3.2877
39	.4826	.1719	2.0804	1.8114	.2922	4.9973	7.2984	3.4125
40	.4884	.1781	2.0428	2.1159	.3413	5.1405	7.4358	3.5557
41	.4915	.1825	2.0284	2.3331	.3763	5.2229	7.4013	3.6381
42	.4802	.1674	2.0305	1.6470	.2656	4.8829	7.2009	3.2981
43	.4825	.1722	2.0254	1.7970	.2898	4.9876	7.2796	3.4028
44	.4872	.1774	2.0164	2.0501	.3307	5.0967	7.4005	3.5119
45	.4889	.1791	2.0110	2.1088	.3401	5.1389	7.4269	3.5541
46	.4937	.1841	2.0031	2.4179	.3900	5.2380	7.5523	3.6532
47	.4785	.1692	1.9964	1.6465	.2656	4.9361	7.1900	3.3513
48	.4862	.1765	1.9982	1.9391	.3128	5.0525	7.3461	3.4677
49	.4916	.1806	1.9961	2.1938	.3538	5.1773	7.4626	3.5925
50	.4996	.1899	1.9866	2.8070	.4527	5.3808	7.6888	3.7960

F3 = (TAJ W G * D **2)/(4 * RHO* * NU* **2)

F5 = (TAU W G * H **2)/(4 * RHO* * NU* **2)

F4 = ((DELTA P)P * D **2)/(4 * RHO* * NU* **2)

TABLE II (CONT.)

CALCULATED RESULTS

TEST NO.	LOG F6	LOG F7	RE THETA * 10 ** -4	(CF)G * 10 ** 3	(CF)P * 10 ** 3	(CF)F * 10 ** 3	(CF)VD * 10 ** 3
1	5.5535	5.7446	2.0088	1.34246	1.4599	1.2334	1.3211
2	5.6230	5.8113	2.1076	1.24488	1.4683	1.2547	1.3220
3	5.7969	5.9812	2.4681	1.19678	1.4487	1.2662	1.2930
4	5.8860	6.0719	2.6290	1.23874	1.4449	1.2679	1.2928
5	5.9882	6.1736	2.8926	1.25687	1.4307	1.2677	1.2752
6	6.0939	6.2790	3.1981	1.23418	1.4145	1.2650	1.2573
7	6.1451	6.3267	3.3605	1.24254	1.3946	1.2616	1.2492
8	6.4453	6.4453	3.8326	1.24929	1.3572	1.2425	1.2156
9	5.7822	5.9642	2.3222	1.23516	1.4716	1.2904	1.3350
10	6.0585	6.2373	3.0581	1.27208	1.4177	1.2801	1.2725
11	5.7878	5.9755	2.3226	1.25651	1.4798	1.2833	1.3418
12	6.0834	6.2610	3.9965	1.25336	1.3593	1.2582	1.2203
13	6.4093	6.5432	6.6989	1.08782	1.0787	1.0969	1.1270
14	6.7856	6.9215	9.4223	.99624	1.0221	1.0683	1.0934
15	6.8537	6.9957	9.9971	1.00360	1.0138	1.0526	1.0932
16	6.8940	7.0317	10.3447	1.13441	.9990	1.0498	1.0920
17	6.8180	6.9662	10.1477	1.04229	1.0138	1.0366	1.0629
18	6.9659	7.1102	11.3185	1.04152	.9882	1.0280	1.0691
19	7.0894	7.2327	12.4245	1.03697	.9645	1.0189	1.0729
20	7.1891	7.3333	13.6269	1.02214	.9479	1.0077	1.0666
21	7.2652	7.4045	14.5678	1.02407	.9273	1.0016	1.0625
22	7.1274	7.2645	13.5819	1.03872	.9595	1.0288	1.0261
23	7.2336	7.3761	14.7650	1.04996	.9436	1.0102	1.0312
24	7.3170	7.4594	15.8291	1.02970	.9306	1.0035	1.0300
25	7.4452	7.5885	17.7880	1.07405	.9120	.9921	1.0213
26	6.6101	6.7385	7.4402	1.11781	1.0331	1.0801	1.1719
27	6.8654	6.9941	9.6750	.99428	.9882	1.0548	1.1247
28	6.7210	6.8567	9.2795	1.01531	1.0208	1.0615	1.0671
29	6.8030	6.9368	9.6918	1.13958	1.0104	1.0621	1.0815
30	6.8394	6.9684	9.8675	1.04793	.9992	1.0635	1.0888
31	6.9414	7.0756	10.8506	1.04728	.9851	1.0466	1.0807
32	7.0409	7.1726	11.9242	1.05288	.9657	1.0396	1.0700
33	7.1151	7.2492	12.7809	1.05287	.9539	1.0285	1.0639
34	7.2012	7.3323	13.7853	1.05004	.9372	1.0238	1.0589
35	7.0710	7.2085	13.1270	1.07738	.9841	1.0499	1.0004
36	7.1563	7.2979	13.9528	1.06770	.9748	1.0387	.9913
37	7.2524	7.3872	15.0997	1.06666	.9492	1.0335	.9799
38	5.4547	5.5913	3.7020	1.12658	1.2117	1.1320	1.2325
39	5.5817	5.7136	4.0975	1.16462	1.1998	1.1434	1.2098
40	5.7242	5.8510	4.5989	1.20875	1.1784	1.1481	1.1842
41	5.8165	5.8165	4.9921	1.21042	1.1620	1.1526	1.1668
42	5.4769	5.6161	3.5842	1.10909	1.2236	1.1395	1.2432
43	5.5638	5.6948	3.8792	1.18849	1.2058	1.1498	1.2281
44	5.6892	5.8157	4.3719	1.17944	1.1851	1.1520	1.2064
45	5.7167	5.8421	4.4733	1.23159	1.1838	1.1560	1.2039
46	5.8459	5.9675	5.0616	1.18188	1.1617	1.1552	1.1816
47	5.4738	5.6052	3.4775	1.27598	1.2188	1.1524	1.2651
48	5.6347	5.7613	4.0824	1.20153	1.1999	1.1603	1.2288
49	5.7513	5.8778	4.5839	1.25309	1.1839	1.1569	1.2054
50	5.9854	6.1048	5.7603	1.22828	1.1414	1.1534	1.1626

F6 = (DELTA P F * H **2)/(4 * RHO* * NU* **2)

F7 = (($\overline{\text{DELTA P}}$)P * H **2)/(4 * RHO* * NU* **2)

TABLE II (CONT.)

CALCULATED RESULTS

TEST NO.	ME ME	DELTA_PF QE	RHO_E RHO*	R*ED * 10 ** -4	R*EH * 10 ** -4	LOG F3	LOG F4	LOG F5
51	.5016	.1931	1.9770	3.0886	.4982	5.2141	7.7732	3.6293
52	.5054	.1960	1.9705	3.4689	.5595	5.5589	7.8793	3.9741
53	.4925	.1825	1.9674	2.2914	.3696	5.1984	7.4958	3.6136
54	.4990	.1908	1.9621	2.8611	.4615	5.3968	7.6989	3.8120
55	.5349	.2161	1.9438	8.4867	1.3688	6.1881	8.6997	4.6033
56	.5384	.2168	1.9181	9.2046	1.4846	6.3033	8.7700	4.7185
57	.5363	.2193	1.9071	9.4538	1.5248	6.2641	8.7874	4.6793
58	.5391	.2203	1.8962	10.2919	1.6600	6.3517	8.8632	4.7669
59	.5356	.2182	1.9891	9.4203	1.5194	6.2809	8.8015	4.6961
60	.5383	.2227	1.9465	10.5154	1.6960	6.3980	8.8918	4.8132
61	.5424	.2258	1.9275	11.3877	1.8367	6.5173	8.9635	4.9325
62	.5417	.2271	1.9024	12.0531	1.9440	6.5196	9.0060	4.9348
63	.5409	.2219	2.0015	11.5743	1.8668	6.5051	8.9916	4.9203
64	.5043	.1925	2.0576	3.3230	.5360	5.4390	7.8587	3.8542
65	.5116	.1989	2.0528	4.2862	.6913	5.6815	8.0913	4.0967
66	.5263	.2110	1.9847	6.8051	1.0976	6.0573	8.5028	4.4725
67	.5328	.2179	1.9352	8.9912	1.4502	6.2361	8.7445	4.6513
68	.5362	.2187	1.8886	10.0102	1.6145	6.3177	8.8327	4.7329
69	.5408	.2208	1.8441	10.9720	1.7697	6.4024	8.9093	4.8176
70	.5426	.2247	1.7951	11.9656	1.9299	6.4674	8.9759	4.8826
71	.5222	.2074	1.8671	5.5105	.8888	5.8537	8.2861	4.2689
72	.5232	.2056	2.0654	6.0189	.9708	5.9593	8.4083	4.3745
73	.5338	.2145	2.0021	8.7144	1.4055	6.2695	8.7327	4.6847
74	.5406	.2231	1.9376	11.0568	1.7834	6.4317	8.9373	4.8469
75	.5451	.2257	1.8925	12.1540	1.9603	6.5145	9.0164	4.9297
76	.4931	.1924	2.0553	4.2311	.6824	5.6864	8.0485	4.1016
77	.4990	.1962	1.9976	4.7448	.7653	5.7821	8.1461	4.1973
78	.5026	.1984	1.9718	5.1802	.8355	5.8497	8.2229	4.2649
79	.5055	.2034	1.9386	5.7048	.9201	5.9213	8.3043	4.3365
80	.5074	.2039	1.9211	6.1197	.9870	5.9789	8.3646	4.3941
81	.5099	.2078	1.8952	6.6658	1.0751	6.0375	8.4373	4.4527
82	.5148	.2104	1.8726	7.5376	1.2157	6.1408	8.5471	4.5560
83	.4816	.1810	1.9561	2.5563	.4123	5.2584	7.5690	3.6736
84	.4969	.1972	1.9171	4.1306	.6662	5.6571	8.0041	4.0723
85	.5008	.1967	1.8917	4.4353	.7154	5.7260	8.0669	4.1412
86	.4913	.1891	2.0818	3.8894	.6273	5.6374	7.9779	4.0526
87	.4953	.1937	2.0323	4.4530	.7182	5.7487	8.0920	4.1639
88	.5028	.1990	1.9780	5.3386	.8611	5.8891	8.2508	4.3043
89	.5051	.2018	1.9527	5.7730	.9311	5.9402	8.3172	4.3554
90	.5101	.2042	1.9236	6.3798	1.0290	6.0109	8.4060	4.4261
91	.5130	.2070	1.9019	6.8898	1.1113	6.0752	8.4727	4.4904
92	.5158	.2080	1.8831	7.4092	1.1950	6.1229	8.5364	4.5381
93	.5164	.2106	1.8695	7.9112	1.2760	6.1877	8.5910	4.6029
94	.5191	.2108	1.8511	8.4587	1.3643	6.2411	8.6494	4.6563
95	.5218	.2131	1.8344	9.8146	1.5830	6.3706	8.7792	4.7858
96	.4639	.1634	2.0714	1.7705	.2856	4.9403	7.2534	3.3555
97	.4749	.1700	2.0513	2.0245	.3265	5.0377	7.3746	3.4529
98	.4810	.1742	2.0328	2.3224	.3746	5.1910	7.5011	3.6062
99	.4829	.1767	2.0154	2.4645	.3975	5.2195	7.5525	3.6347
100	.4897	.1821	1.9993	2.7081	.4368	5.3203	7.6430	3.7355

F3 = (TAU W G * D **2)/(4 * RHO* * NU* **2)   F5 = (TAU W G * H **2)/(4 * RHO* * NU* **2)

F4 = ((DELTA P)P * D **2)/(4 * RHO* * NU* **2)

TABLE II (CONT.)

CALCULATED RESULTS

TEST NO.	LOG F6	LOG F7	RE THETA * 10 ** -4	(CF)G * 10 ** 3	(CF)P * 10 ** 3	(CF)F * 10 ** 3	(CF)VD * 10 ** 3
51	6.0734	6.1884	6.2556	1.24399	1.1214	1.1517	1.1503
52	6.1794	6.2945	6.9487	1.22167	1.1024	1.1420	1.1328
53	5.7874	5.9110	4.6591	1.22301	1.1762	1.1595	1.2141
54	5.9986	6.1141	5.7389	1.24196	1.1351	1.1573	1.1735
55	6.9930	7.1149	18.7831	.88126	.9619	1.0518	.9744
56	6.9590	7.1852	19.8378	.98969	.9529	1.0395	.9757
57	7.0847	7.2026	20.1572	.86221	.9414	1.0457	.9776
58	7.1581	7.2784	21.6555	.89515	.9295	1.0337	.9712
59	7.0978	7.2167	21.5914	.86541	.9349	1.0375	.9377
60	7.1927	7.3070	23.0965	.92940	.9185	1.0367	.9430
61	7.2637	7.3787	24.5390	1.05328	.9126	1.0347	.9414
62	7.3099	7.4212	25.3430	.95766	.8985	1.0304	.9462
63	7.2866	7.4068	26.6989	.95464	.8999	1.0118	.9048
64	6.1529	6.2739	8.5730	.96753	1.1042	1.1280	1.0618
65	6.3874	6.5065	10.8834	1.01880	1.0588	1.1071	1.0231
66	6.7998	6.9180	15.9104	.99324	.9886	1.0717	.9863
67	7.0448	7.1597	19.8354	.88088	.9414	1.0483	.9707
68	7.1291	7.2479	21.0143	.87864	.9282	1.0328	.9791
69	7.2025	7.3245	21.9551	.91012	.9221	1.0259	.9893
70	7.2737	7.3911	22.7056	.91306	.9097	1.0275	1.0034
71	6.5826	6.7013	11.7114	1.00754	1.0395	1.1055	1.0825
72	6.6992	6.8235	15.1229	.97356	1.0054	1.0677	.9653
73	7.0246	7.1479	20.3574	.98074	.9478	1.0362	.9441
74	7.2352	7.3525	24.1504	.91259	.9138	1.0291	.9405
75	7.3122	7.4316	25.3607	.93556	.9069	1.0236	.9499
76	6.3621	6.4637	12.1786	1.05601	.9964	1.0767	1.0037
77	6.4578	6.5613	12.9384	1.07708	.9906	1.0750	1.0147
78	6.5333	6.6381	13.7584	1.06956	.9817	1.0691	1.0144
79	6.6205	6.7195	14.6366	1.05780	.9687	1.0750	1.0168
80	6.6786	6.7798	15.4047	1.05916	.9582	1.0639	1.0153
81	6.7553	6.8525	16.3319	1.03564	.9466	1.0661	1.0161
82	6.8622	6.9623	17.9885	1.03985	.9331	1.0541	1.0097
83	5.8764	5.9842	6.9320	1.13474	1.1003	1.1277	1.1413
84	6.3217	6.4193	10.5776	1.11036	1.0257	1.1135	1.0797
85	6.3766	6.4821	11.0444	1.14378	1.0221	1.0972	1.0822
86	6.2871	6.3931	11.5057	1.10231	1.0108	1.0760	1.0039
87	6.4046	6.5072	12.5724	1.11130	.9923	1.0739	1.0071
88	6.5622	6.6660	14.2598	1.09926	.9741	1.1248	1.0066
89	6.6305	6.7324	15.0357	1.07114	.9636	1.0640	1.0077
90	6.7159	6.8212	16.1044	1.04779	.9566	1.0565	1.0079
91	6.7837	6.8879	16.9947	1.05370	.9478	1.0550	1.0078
92	6.8446	6.9516	17.9111	1.02700	.9398	1.0459	1.0069
93	6.9039	7.0062	18.8308	1.05340	.9263	1.0454	1.0045
94	6.9581	7.0646	19.7234	1.05227	.9196	1.0338	1.0047
95	7.0879	7.1944	22.3684	1.06284	.8933	1.0154	.9921
96	5.5378	5.6686	6.1501	1.07371	1.1527	1.0974	1.1173
97	5.6671	5.7898	6.8841	1.03848	1.1350	1.1096	1.1044
98	5.7931	5.9163	7.7391	1.13283	1.1201	1.1056	1.0896
99	5.8472	5.9677	8.0733	1.08351	1.1117	1.1082	1.0885
100	5.9386	6.0582	8.7147	1.14062	1.1204	1.1191	1.0809

F6 = (DELTA P F * H **2)/(4 * RHO* * NU* **2)

F7 = (($\overline{\text{DELTA P}}$)P * H **2)/(4 * RHO* * NU* **2)

TABLE II (CONT.)

CALCULATED RESULTS

TEST NO.	UE ME	DELIA_PF QE	RHO_E RHO*	R*ED * 10 ** -4	R*EH * 10 ** -4	LOG F3	LOG F4	LOG F5
101	.4928	.1857	1.9831	3.1416	.5067	5.4453	7.7739	3.8605
102	.4838	.1863	1.9721	3.3187	.5353	5.4381	7.8121	3.8533
103	.4923	.1923	1.9316	3.9390	.6353	5.5854	7.9582	4.0006
104	.5017	.1912	1.9193	4.4571	.7189	5.6740	8.0792	4.0892
105	.5025	.1932	1.8936	4.8539	.7829	5.7534	8.1486	4.1686
106	.5058	.1975	1.8784	5.2542	.8475	5.8163	8.2197	4.2320
107	.5070	.1978	1.8673	5.4730	.8827	5.8893	8.2546	4.3050
108	.5090	.1961	1.8570	5.8175	.9383	5.8904	8.3086	4.3056
109	.5095	.2048	1.8448	6.2496	1.0080	5.9540	8.3688	4.3692
110	.4976	.1923	2.0247	5.3957	.8703	5.8648	8.2612	4.2800
111	.5056	.1956	1.9647	6.1897	.9983	5.9580	8.3812	4.3732
112	.5080	.1997	1.9310	6.7852	1.0944	6.0392	8.4575	4.4544
113	.5104	.2039	1.9095	7.3190	1.1805	6.0876	8.5227	4.5028
114	.5134	.2070	1.8823	8.0323	1.2955	6.1645	8.6021	4.5797
115	.5148	.2086	1.8630	8.6069	1.3882	6.2109	8.6602	4.6261
116	.5182	.2095	1.8412	9.1228	1.4714	6.3113	8.7113	4.7265
117	.5198	.2110	1.8275	9.4969	1.5318	6.3099	8.7456	4.7251
118	.5224	.2158	1.8092	10.6034	1.7102	6.3895	8.8413	4.8047
119	.5272	.2143	1.7954	11.6502	1.8791	6.4589	8.9277	4.8741
120	.5135	.2080	1.9780	9.5039	1.5329	6.3206	8.7703	4.7358
121	.5207	.2122	1.9094	11.0266	1.7785	6.4252	8.8960	4.8404
122	.5249	.2150	1.8707	12.3643	1.9942	6.5061	8.9933	4.9213
123	.5292	.2185	1.8311	13.9113	2.2438	6.5949	9.0937	5.0101
124	.5324	.2177	1.7881	15.2802	2.4645	6.6704	9.1701	5.0856
125	.5353	.2226	1.7648	16.6554	2.6864	6.7836	9.2439	5.1988
126	.5230	.2187	1.9184	12.9531	2.0892	6.5806	9.0417	4.9958
127	.5337	.2219	1.8804	14.9989	2.4192	6.6958	9.1778	5.1110
128	.5366	.2206	1.8314	16.3848	2.6427	6.7598	9.2478	5.1750
129	.5378	.2223	1.8123	18.2702	2.9468	6.8470	9.3398	5.2622
130	.5421	.2248	1.8056	18.8899	3.0468	6.8738	9.3742	5.2890
131	.5367	.2148	1.9155	16.7385	2.6998	6.7911	9.2862	5.2063
132	.5427	.2180	1.8255	20.0186	3.2288	6.9466	9.4302	5.3618
133	.4664	.1701	1.9794	2.5794	.4160	5.2456	7.5541	3.6608
134	.4743	.1771	1.9366	2.9391	.4740	5.3404	7.6725	3.7556
135	.4765	.1827	1.9217	3.3457	.5396	5.4502	7.7856	3.8654
136	.4812	.1858	1.8789	3.7512	.6050	5.5244	7.8841	3.9396
137	.4855	.1913	1.8791	4.2042	.6781	5.6290	7.9907	4.0442
138	.4907	.1916	1.8382	4.6054	.7428	5.7065	8.0694	4.1217
139	.4949	.1949	1.8493	4.9941	.8055	5.7741	8.1500	4.1893
140	.4968	.1901	1.8573	5.3183	.8578	5.8200	8.2098	4.2352
141	.4993	.1919	1.7023	6.4813	1.0454	5.9873	8.3480	4.4025
142	.5002	.1921	1.8242	5.8410	.9421	5.8975	8.2892	4.3127
143	.5025	.1948	1.8086	6.2586	1.0095	5.9565	8.3495	4.3717
144	.5033	.1987	1.8140	6.7903	1.0952	6.0255	8.4230	4.4407
145	.5052	.1999	1.7359	7.1551	1.1540	6.0646	8.4651	4.4798
146	.5094	.1994	1.7627	7.6204	1.2291	6.1076	8.5182	4.5228
147	.5090	.2020	1.7539	8.0603	1.3000	6.1574	8.5672	4.5726
148	.5092	.2025	1.7561	8.4672	1.3657	6.2011	8.6107	4.6163
149	.5130	.2040	1.7429	8.9787	1.4482	6.2413	8.6649	4.6571

F3 = (TAU W G * D **2)/(4 * RHO* * NU* **2)

F5 = (TAU W G * H **2)/(4 * RHO* * NU* **2)

F4 = ((DELTA P)P * D **2)/(4 * RHO* * NU* **2)

TABLE II (CONT.)

CALCULATED RESULTS

TEST NO.	LOG F6	LOG F7	RE THETA * 10 ** -4	(CF)G * 10 ** 3	(CF)P * 10 ** 3	(CF)F * 10 ** 3	(CF)VD * 10 ** 3
101	6.0727	6.1891	9.9076	1.13956	1.0820	1.1081	1.0646
102	6.1192	6.2273	11.2075	1.01009	1.0525	1.1002	1.0475
103	6.2729	6.3734	12.7395	1.02771	1.0212	1.0978	1.0418
104	6.3748	6.4944	14.1718	.99042	1.0222	1.0668	1.0292
105	6.4477	6.5638	15.0178	1.01638	1.0037	1.0610	1.0300
106	6.5224	6.6349	15.9794	1.01164	.9951	1.0664	1.0260
107	6.5561	6.6698	16.4471	1.10974	.9894	1.0481	1.0259
108	6.6028	6.7238	17.2690	.98896	.9808	1.0403	1.0223
109	6.6810	6.7840	18.2891	.99869	.9649	1.0677	1.0182
110	6.5665	6.6764	18.6930	.99411	.9513	1.0283	.9485
111	6.6802	6.7964	20.2536	.96480	.9468	1.0202	.9577
112	6.7615	6.8727	21.4625	.98474	.9336	1.0231	.9614
113	6.8313	6.9379	22.6429	.95690	.9243	1.0282	.9615
114	6.9126	7.0173	24.1415	.96201	.9125	1.0256	.9624
115	6.9713	7.0754	25.3300	.94202	.9017	1.0199	.9628
116	7.0188	7.1265	26.2378	1.06913	.8993	1.0139	.9154
117	7.0535	7.1608	26.9135	.99079	.8955	1.0134	.9678
118	7.1545	7.2565	29.3767	.96421	.8785	1.0132	.9623
119	7.2301	7.3429	31.7129	.94431	.8714	.9897	.9569
120	7.0822	7.1855	30.9035	.93683	.8679	.9923	.8940
121	7.2046	7.3112	33.5037	.91735	.8586	.9853	.9066
122	7.3010	7.4085	36.0461	.89717	.8466	.9775	.9107
123	7.4011	7.5089	38.8593	.88822	.8350	.9715	.9152
124	7.4707	7.5853	40.7143	.89704	.8257	.9533	.9250
125	7.5494	7.6591	43.2224	.99284	.8161	.9576	.9262
126	7.3598	7.4569	39.1284	.94620	.8285	.9814	.8818
127	7.4846	7.5930	43.6195	.93864	.8275	.9684	.8818
128	7.5474	7.6630	45.2334	.93597	.8190	.9494	.8943
129	7.6408	7.7550	49.3672	.92979	.7998	.9373	.8897
130	7.6730	7.7894	50.5693	.92848	.8043	.9410	.8898
131	7.5738	7.7014	49.9808	.92155	.8100	.9190	.8527
132	7.7148	7.8454	54.3929	.96700	.7923	.9042	.8733
133	5.8685	5.9693	9.8052	1.06935	1.0366	1.0634	1.0682
134	5.9838	6.0877	10.7007	1.04704	1.0337	1.0774	1.0693
135	6.1066	6.2008	11.9813	1.04872	1.0079	1.0820	1.0561
136	6.2036	6.2993	12.8397	1.01154	.9978	1.0767	1.0609
137	6.3152	6.4059	14.3644	1.02525	.9833	1.0818	1.0427
138	6.3854	6.4846	15.0539	1.04399	.9805	1.0665	1.0510
139	6.4659	6.5652	16.4891	1.03107	.9734	1.0660	1.0322
140	6.5117	6.6250	17.6150	1.00607	.9632	1.0294	1.0184
141	6.6496	6.7632	18.2208	1.08656	.9326	1.0076	1.0792
142	6.5896	6.7044	18.6834	1.01512	.9529	1.0220	1.0227
143	6.6521	6.7647	19.6388	1.02152	.9443	1.0225	1.0212
144	6.7328	6.8382	21.3963	1.01431	.9263	1.0244	1.0062
145	6.7741	6.8803	21.8461	1.01526	.9216	1.0212	1.0141
146	6.8220	6.9334	22.6464	1.00132	.9211	1.0078	.9303
147	6.8742	6.9824	23.6851	1.00865	.9068	1.0092	1.0149
148	6.9187	7.0259	24.9096	1.00961	.8953	1.0020	1.0066
149	6.9694	7.0801	25.9954	.99369	.8941	.9979	1.0057

F6 = (DELTA P F * H **2)/(4 * RHO* * NU* **2)

F7 = ((DELTA P)P * H **2)/(4 * RHO* * NU* **2)

☆U.S.Government Printing Office: 1978 — 757-080/125